DOKUZ EYLÜL UNIVERSITY
GRADUATE SCHOOL OF NATURAL AND APPLIED SCIENCES

EFFECTS OF CLIMATE CHANGE IN ZANZIBAR AND SUSTAINABLE LAND MANAGEMENT

by
Ibrahim Khalid MAMBO

September, 2016
İZMİR

EFFECTS OF CLIMATE CHANGE IN ZANZIBAR AND SUSTAINABLE LAND MANAGEMENT

A Thesis Submitted to the
Graduate School of Natural and Applied Sciences of Dokuz Eylül University in Partial Fulfilment of the Requirements for the Degree of Master of Science in Geographical Information Systems

by
Ibrahim Khalid MAMBO

September, 2016
İZMİR

M.Sc THESIS EXAMINATION RESULT FORM

We have read the thesis entitled **"EFFECTS OF CLIMATE CHANGE IN ZANZIBAR AND SUSTAINABLE LAND MANAGEMENT"** completed by **IBRAHIM KHALID MAMBO** under supervision of **ASST. PROF. DR. HÜSNÜ ERONAT** and we certify that in our opinion it is fully adequate, in scope and in quality, as a thesis for the degree of Master of Science.

Asst. Prof. Dr. Hüsnü ERONAT

Supervisor

Prof. Dr. Doğan YASAN	Doç. Dr. M. Kirami Ölgen
(Jury Member)	(Jury Member)

Prof.Dr. Ayşe OKUR

Director

Graduate School of Natural and Applied Sciences

ACKNOWLEDGMENTS

I would like to take this opportunity to express my thanks and gratitude to my supervisor Asst. Prof. Dr. Hüsnü Eronat, for his valuable efforts, valuable assistance and advice that he gave me in conducting this thesis. I would also like to mention Prof. Dr. Doğan Yaşar for his constant support and help throughout the writing of this thesis.

I would also like to convey my thanks to my family especially to my mother for their support and motivation during my study period.

Ibrahim Khalid MAMBO

EFFECTS OF CLIMATE CHANGE IN ZANZIBAR AND SUSTAINABLE LAND MANAGEMENT

ABSTRACT

The concept of climate change is very crucial in today's world as far as the sustainability of our planet is concerned. We have been witnessing unexpected rapid and erratic changes of our planet's climate over the past few decades. This is also coupled with the occurrence of extreme weather conditions throughout the world as a result of these changes. Our planet Earth has also witnessed major floods, droughts and a steep climb in global temperatures.

Social factors, such as increasing population growth and rapid urbanization and industrialization have contributed to an increased pressure on land resources and the environment worldwide. Unprecedented deforestation and land degradation have been taking place from savannah grasslands to the deep rainforests, and the oil-rich desserts to the megacities. The change in our climate, with the help of contributing social factors, has exacerbated the pressure that our land resources have been facing.

The aim of this thesis is to investigate the effects of climate change and changes in land covers for sustainable management of land in Zanzibar Islands using remote sensing techniques and Geographic Information Systems (GIS). With the help of remotely sensed data from satellite systems and locally gathered metrological data, a relationship between land cover changes and climate change in Zanzibar.

The study is deemed to be useful in providing a way for planners and researchers to formulate policies and current policy adaptation in preservation and management of land resources in Zanzibar.

Keywords: Climate change, land cover, GIS, Zanzibar, remote sensing

ZANZİBAR DA İKLİM DEĞİSİKLİĞİNİN ETKİLERİ VE SÜRDÜRÜLEBİLİR ARAZİ YÖNETİMİ

ÖZ

Günümüz dünyasında, gezegenimizin sürdürülebilirliği göz önünde bulundurulduğunda iklim değişikliği oldukça önemli bir kavramdır. Geçtiğimiz on yıllarda gezegenimizin ikliminde ani ve düzensiz değişiklikler gözlemledik. Bu değişikliklerin bir sonucu olarak dünya çapında şiddetli hava şartları meydana geldi. Gezegenimiz Dünya aynı zamanda büyük sellere, kuraklıklara ve küresel sıcaklıkta sert bir yükselişe tanıklık etti.

Nüfus artışı, hızlı kentleşme ve sanayileşme gibi toplum faktörleri; toprak kaynaklarına ve çevreye olan baskıyı arttırdı. Daha önce görülmemiş bir şekilde; ormansızlaşma ve arazi bozulumu, terk edilmiş çayırlardan yağmur ormanlarının derinliklerine ve petrol zengini çöllerden büyük şehirlere taşındı.

Bu tezin amacı arazinin sürdürülebilir yönetimi için Zanzibar adalarındaki iklim değişikliğinin etkilerini ve arazi örtüsü değişikliklerini, Uzaktan Algılama teknikleri ve Coğrafi Bilgi Sistemleri (CBS) kullanarak incelemektir.

Uydu sistemlerinden sağlanan uzaktan algılanmış verilerin ve yerel olarak elde edilen metrolojik verilerin ışığında, bu tez Zanzibar'daki arazi örtüsü değişiklikleri ve iklim değişikliği arasında bir ilişki kurmayı amaçlar.

Bu çalışma, planlamacılar ve araştırmacılara Zanzibar'ın toprak kaynaklarının korunması ve yönetimi için politika oluşturmalarında ayrıca güncel politikalarında yardımcı olacaktır.

Anahtar Kelimeler: İklim değişikliği, arazi örtüsü, CBS, Zanzibar, uzaktan algılama

CONTENTS

Pages

THESIS EXAMINATION RESULT FORM ii
ACKNOWLEDGMENTS iii
ABSTRACT iv
ÖZ v
LIST OF FIGURES x
LIST OF TABLES xii

CHAPTER ONE - INTRODUCTION 1

1.1 Background and Study Objective 1
1.2 Remote Sensing Basics 3
1.2.1 Pre-processing of Data 6
1.2.1.1 Radiometric Correction 7
1.2.1.2 Atmospheric Correction 8
1.2.1.3 Geometric Correction 9
1.2.2 Vegetation Indices 10
1.2.3 Supervised Classification 11
1.2.4 Unsupervised Classification 11
1.2.5 Change Detection Techniques 11
1.2.5.1 Image Differencing 12
1.2.5.2 Image Ratioing 12
1.2.5.3 Image Regression 13
1.2.5.4 Vegetation Index Differencing 13
1.2.5.5 Post-Classification Comparison 14
1.2.5.6 Principal Component Analysis (PCA) 14
1.3 Climate Change 14
1.3.1 Climate Change Causes 15
1.3.1.1 Tectonic Plates 15
1.3.1.2 Volcanism and Meteors 18

1.3.1.2.1 Tombora Volcano ... 20
1.3.1.2.2 El Chichon volcano ... 20
1.3.1.2.3 Pinatubo Volcano ... 22
1.3.1.3 Solar Energy Fluctuation ... 22
1.3.1.3.1 The Sun ... 23
1.3.1.3.2 Sunspots ... 24
1.3.1.3.3 Sunspot Cycle ... 27
1.3.1.3.4 Correlation between Solar Energy and Temperatures ... 30
1.3.1.4 Human Activities ... 31
1.3.2 Climate Change Indicators ... 31
1.3.2.1 Air Temperature over Land and Sea and Global Precipitation ... 31
1.3.2.2 Heat trapping gases ... 32
1.3.2.3 Arctic Sea Level ... 33
1.3.2.4 Ocean Heat ... 34
1.3.2.5 Snow, Glaciers and Ice Sheet ... 35
1.3.2.6 Sea Level ... 36
1.3.2.7 Ocean Acidification ... 37
1.3.3 Climate Change Impact ... 38
1.3.3.1 Water ... 38
1.3.3.2 Health ... 39
1.3.3.3 Agriculture ... 39
1.3.3.4 Ecosystems ... 40
1.3.3.5 Coastal Zones ... 41
1.3.3.6 Settlements, Industry, Infrastructure and Society ... 41

CHAPTER TWO - STUDY AREA AND DATA DESCRIPTION ... 43

2.1 Study Area ... 43
2.1.1 Population ... 43
2.1.2 Climate ... 43
2.1.3 Topography ... 45
2.1.4 Vegetation and Drainage ... 47

2.2 Climate Change in Unguja 47
2.2.1 Current State of Climate Change in Unguja Island 47
2.2.1.1 Climate Change Indicators in Unguja Island 48
2.2.1.1.1 Temperature 48
2.2.1.1.2 Rainfall 49
2.2.1.1.3 Sea Level Rise 50
2.2.1.2 Climate Change Impact in Unguja Island 51
2.2.1.2.1 Coastal Zones 51
2.2.1.2.2 Fishery and Marine Ecosystem 52
2.2.1.2.3 Agriculture 52
2.2.1.2.4 Health 53
2.2.1.2.5 Water Resources 53
2.2.1.2.6 Forests 53
2.2.1.2.7 Infrastructure 53
2.2.1.3 Adaptation and Mitigation 53
2.2.2 Future Trend 54
2.3 Data Description 55
2.3.1 Remote Sensing Data 56
2.3.1.1 Landsat Mission 56
2.3.1.1.1 Satellite Acquisitions 57
2.3.1.1.2 Sensors and Band Designations 58
2.3.1.1.3 Landsat Data Products and Processing 59
2.3.1.1.4 Obtaining Landsat Data Products 60
2.3.1.2 Characteristics of Data Used for this Study 60
2.3.1.3 Pre-processing of Landsat Imagery 61
2.3.2 Climate Data 61
2.3.3 Other Data 61

CHAPTER THREE - METHODOLOGY 62

3.1 Radiometric and Atmospheric Correction 62
3.2 Development of Indices 63

3.2.1 Normalized Difference Vegetation Index (NDVI).................................. 63
3.2.2 Normalized Difference Built-Up Index (NDBI) 64
3.3 Landsat Image Classification.. 67
3.4 Estimation of Land Surface Temperature (LST) using Landsat TM Data (NDVI method).. 69
3.4.1 Land Surface Emissivity (LSE)... 69
3.4.2 Calculating Brightness Temperature 72
3.4.3 Estimation of Land Surface Temperature 72

CHAPTER FOUR - RESULTS AND ANALYSIS 75

4.1 LST, NDVI and NDBI Relationship 75
4.2 Land-cover Types and LST Relationship... 77

CHAPTER FIVE - CONCLUSIONS AND DISCUSSION.................................. 80

REFERENCES.. 83

APPENDICES 91

LIST OF FIGURES

Page

Figure 1.1 From Pangea to the present 16
Figure 1.2 The areas covered by glacial ice in Pangea their present location 17
Figure 1.3 The explosion of Mount Etna as seen from the space 19
Figure 1.4 Solar radiation chnages and the effect of the volcanos..................... 21
Figure 1.5 The Sun..................... 23
Figure 1.6 Sunspots..................... 24
Figure 1.7 Sunspots..................... 25
Figure 1.8 Sunspots magnetism 26
Figure 1.9 Flare explosion in the Sun 26
Figure 1.10 A typical sunspot cycle..................... 27
Figure 1.11 Butterfly diagram showing paired Spörer's law behavior 28
Figure 1.12 Changes in radiation from the Sun (Rohde, 2006) 30
Figure 1.13 Climate change indicators. 32
Figure 1.14 Worldwide emissions of greenhouse gases 33
Figure 1.15 Arctic sea ice extent..................... 34
Figure 1.16 Changes in ocean heat content between 1955 and 2014..................... 35
Figure 1.17 The cumulative change in mass balance of ice sheets..................... 36
Figure 1.18 Cumulative changes in sea level for the world’s oceans since 1880...... 37
Figure 1.19 Changes in ocean acidity 38
Figure 2.1 Map of Unguja Island showing the study area 44
Figure 2.2 Average Annual Climate on Unguja island..................... 45
Figure 2.3 Map showing a topographyof Unguja island..................... 46
Figure 2.4 Average maximum temperature on Unguja island, 1983 - 2010.............. 48
Figure 2.5 Average minimum temperature on Unguja island, 1983 - 2010 49
Figure 2.6 Annual rainfall on Unguja island, 1983 - 2010 50
Figure 2.7 Monthly Mean sea level (mm) on Unguja island, 1984 - 2012................ 51
Figure 2.8 Future climate change prediction on Unguja island 55
Figure 2.9 Timeline and history of the Landsat Missions..................... 57
Figure 3.1 NDVI image of study area using Landsat TM..................... 65

Figure 3.2 NDBI image of the study area using Landsat TM 66
Figure 3.3 Classification of Landsat TM - 2009 image 68
Figure 3.4 Study area emissivity calculated from NDVI image raster 71
Figure 3.5 LST image of the study area 74
Figure 4.1 The relationship between LST and NDBI 75
Figure 4.2 The relationship between LST and NDBI 76
Figure 4.3 The relationship between NDBI and NDVI 77

LIST OF TABLES

Page

Table 2.1 Display and comparison of the Landsat bands and wavelengths............... 59
Table 2.2 The bands of each Landsat satellite and their descriptions. 59
Table 2.3 Landsat data used in this study 60
Table 3.1 LSE classification using NDVI algorithm 70
Table 4.1 Landsat TM - 2009 classification in the study area 78
Table 4.2 Descriptive statistics of LST against land cover/use for the study area..... 79

CHAPTER ONE
INTRODUCTION

1.1 Background and Study Objective

Any sustainable development plan needs to have a relevant and continuously updated data for analysis and better policy formulation that will in turn help in applying suitable strategies for implementation of the plan. This same principle applies to sustainable land management and land related practices. Fortunately, the rapid development of remote sensing systems and readily attainable data produced by these systems and practices can easily assist in creating what is termed as sustainable land management.

The development of sophisticated Geographical Information Systems (GIS) systems and availability of multispectral satellite images, which can be tracked back to the middle of the past century to its application in military and in forest and land use mapping (Chavez, 1996), can be combined and integrated in development and implementation of plans for better land management. These technologies, coupled with the development of powerful GIS software and the development of high-end computing machinery have helped planners and researchers in land and environment management for the sustainability of our planet.

The ever growing world population has created an enormous pressure on energy consumption and on natural resource, especially in coastal areas. The results are land, water and air pollutions as well as deforestation, land degradation and even biodiversity loss (Senga, Kihupi, Liwa, & Kimaro, 2014). Development of industries emitting chemical toxins into the air and the urban expansion all over the world has doubled the impact and consumption of natural resources as well as creating room for poor land use practices.

Humans alone do not pose a challenge to land resources as far as this topic is concerned. Although the effect of the human activities to the atmosphere through toxic emission and greenhouse effect has had its toll on land covers and vegetation in general, the last three decades have witnessed an ever increasing rate in global temperatures, floods and other natural disasters that are associated with climate change (Wilbanks et al., 2007).

The effects of climate change range from human health to coastal erosions, energy sectors to land cover changes and if positive and intentional combating measures are not taken, the backlash will be so severe in the near future.

Climate data has provided a way for scientists to study changes in climate patterns on land and sea surface since the late 1880's (United States Environmenatal Protection Agency [EPA], 2014). This has helped in identification and formulation of models that will help in capturing the future of our climate. Since the changes in climate conditions have a different impact on animals and natural resources, different governments have established task forces and agencies to study weather patterns and formulate strategies and policies that can help with reducing and mitigating the negative consequences resulting from climate change.

One of the effects of climate change is sea level rise. The current level of sea level rise is estimated to be 0.57 to 1.10 m by 2100 (Brown, Kebede & Nicholls, 2011; Jevrejeva, Moore & Grinsted, 2012). Such numbers pose a very serious threat to small islands and low-lying coastal areas.

Climate change can occur due to various reasons, but the observed 20th-century trend is mainly attributed to man-made greenhouse emission (EPA, 2014). Nonetheless, developing countries which suffer from the impacts of climate change contribute very little to these emissions (Paavola & Adger, 2002; Brown, Kebede & Nicholls, 2011). This is partly due to developing countries focuses on poverty eradication programs rather than on curbing climate change. Moreover, such policies require a huge financial budget backing which is not easily justifiable in such countries. Zanzibar is one of those countries that faces challenges in land and coastal resources while at the same time faces huge negative impacts of climate change. It is also an example of developing countries that struggle to have an adaptive capacity in combating the negative consequences of climate change (Nicholls et al., 2007).

These impacts may include a decrease in agricultural production, water resources, coastal zones destruction, even negative effects on human health (EPA, 2014). Lack of adaptive policies and social factors such as population growth and extreme poverty put Africa, as a developing continent, at much higher risk at the receiving end of climate change impacts (Boko et al., 2007). Most economic sectors in developing countries, a case for most African countries, are climate sensitive (Brown, Kebede, & Nicholls, 2011). Sectors such as fishery, agriculture and tourism will be hit the most by the negative effects of climate change (Brown, Hammill & MacLeman, 2007).

Zanzibar, an island with a majority of its population residing in its coastal area, is a characteristic of most coastal areas. Coastal cities tend to have high population densities, thus land resources face huge challenges from land clearing for settlements and farming activities, over-harvesting, pollution and climate change (Senga, Kihupi, Liwa & Kimaro, 2014).

1.2 Remote Sensing Basics

Remote sensing is the science of obtaining information about objects of interest or areas from a distance, typically from aircraft or satellites (NOOA, 2015). The energy reflected from the earth surface is picked out by the sensors mounted either on the satellite systems or an aircraft.

Schowengerdt (2006), defined remote sensing as the measurement of object properties on the earth's surface using data acquired from aircraft and satellites. He further noted that the signals propagated from the object of interest are received by optical or microwave systems. These systems can accomplish the capturing of consistent and repetitive view of the globe that is vital in change detecton and monitoring all scale of measurements and the accompanying human activites.

These changes include and are not limited to assesment of enviromental dynamics and their monitoring, agricultural activities such as monitoring of crop conditions, meteorology as in weather predictions and mapping which includes land use and topography mapping.

In remote sensing, the **sensors** are not in direct contact with the objects or events being observed. The information needs a physical **carrier** to travel from the objects/events to the sensors through an intervening medium.

The most important attributes of remote sensing are:

- Information about an object or area: any remote sensing system focuses on an object of interest on the earth surface. Texture, shape and size are very important attributes in acquiring information about an object of interest and its attributes. These objects of interests reflect energy in wavelengths that are received by recording systems on satellites or aircraft carrying scanning systems.
- Instrument (sensor): Remote sensing systems have specialized instruments for capturing earth imagery, the instruments are called sensors. Most sensors record light wavelength emitted from the sun. The changes of wavelength detected by the sensor provide what is called ‘raw data’. When this data is interpreted, it provides information regarding the real-life phenomenon being investigated. Not all sensors record electromagnetic wavelength from the solar energy, some sensors record sound waves or energy reflected from laser systems.
- Distance (how far is remote?): The idea of remote sensing is acquiring information without direct contact with the object. However, the question is how far is remote? The distance can vary from 1millimeter to thousands of kilometres

It is important to note that the sun is the source of the electromagnetic energy that is recorded in the remote sensing systems or sensors. In general, these systems record images in two ways: (a) Passive sensors: measures naturally available electromagnetic radiation that is reflected or emitted from the surface. These sensors can only record energy that is naturally available. The visible wavelengths from the sun's energy are reflected to the sensor. For the thermal infrared wavelengths, they are absorbed and the re-emitted. The reflection of visible wavelengths only occurs when the sun is illuminating the earth which happens during the daytime. Thermal infrared wavelength can be recorded both during daytime and at night provided that there is a sufficient record energy. (b) Active sensors: bathe terrain or an object of interest in their own energy source and then measure the amount of radiant flux reflected back toward the sensor. However, these sensors generate enormous amount of energy to sufficiently illuminate the object of interest. Laser fluorosensor and a Synthetic Aperture Radar (SAR) are examples of active sensors.

There are four types of resolution associated with satellites systems, namely;

1. Spatial resolution: registration of two remotely sensed images requires both image data to have a same *instantaneous field of view*. Landsat Enhanced Thematic Mapper (ETM+) and Landsat Operational Land Imager (OLI) both collects images at 30m by 30m spatial resolution. Though it is possible to work with two images with different spatial resolution, the requirement is that the image with lower spatial resolution should be resampled to match the one with higher resolution. It should be noted though, for example resampling 30m by 30m Landsat image to 20m by 20m will not yield any additional spectral details (Jensen, 2005).

2. Temporal resolution: This is the ability of a remote sensing system to obtain data at approximately the same time of the day. For example, the temporal resolution for Landsat 8 satellite is 16 days. The advantage of this is to eliminate diurnal sun angle effects that can cause anomalies in the reflectance of the imagery. It is also advised that the image data be acquired on an anniversary i.e. same date and month to minimize seasonal effects such as sun angle and plant phenological differences (Jensen, 2005). Vegetation phenology cycle tends to be different in different seasons of the month.

3. Spectral resolution: Spectral data is recorded in individual pixels for each band of the image data. However, the same pixel will have different spectral response in an image collected at a different date. Remote sensor systems record radiant energy from surfaces to represent spectral characteristics of a particular surface. Different remote sensing systems record energy in a different portion of the electromagnetic spectrum. For instance, Landsat multispectral scanner (MSS) record electromagnetic energy in four multispectral bands in contrast to Landsat Enhanced Thematic Mapper ETM+ which collects data in six visible bands, one thermal infrared band and one broad panchromatic band. Landsat MSS bands 4 green 5 red and 3 NIR can be successfully compared and matched with ETM bands 2 green, 3 red and 4 NIR spectral wise (Jensen, 2005).

4. Radiometric resolution: this is the depth of recorded data in brightness values. 8-bit brightness values range from 0 to 255. An example of a satellite that records at this depth is Landsat ETM. On the other hand, Landsat Operational Land Imager (OLI) records pixel values in 16-bit brightness values, that correspond to 55,000 grey levels (USGS, 2015). When working with two images with different radiometric resolution it is recommended to convert data to apparent surface reflectance to eliminate brightness values compression and decompression problems (Jensen, 2005).

1.2.1 Pre-processing of Data

Data acquired by remote sensing systems is subjected to errors and unwanted artefacts that need to be removed prior to any operation or analysis (Chavez, 1988). The pixels in the recorded image data are prone to geometric and radiometric errors. Radiometric errors may be a result of atmospheric effects, remote sensing instrumentation errors and solar radiation wavelength. The relative motion of scanning systems and the earth might result into skewing of imagery products which is an example of geometric errors. Earth curvature is another source of geometric errors (Richards & Jia, 2006).

Working with images acquired from different dates is essential when performing changes over a period of time. For easiness and effective usage of multi-temporal data, radiometric and geometric corrections are needed (Chavez, 1996).

These errors are categorized into two groups, i.e., internal geometric errors and external geometric errors. It is also essential to identify the nature of these two types of errors which can be either systematic or non-systematic.

Internal geometric errors can be either resulted by the remote systems themselves or rotation of the earth during image acquisition and these errors are mostly systematic. That means they can be corrected using information about the sensor and the time of image acquisition (Jensen, 2005).

External geometric errors can be a result of random movement of spacecraft, such as altitude changes and changes in elevation. Errors can also result from pitch, yaw and roll of the aircraft carrying remote sensing system (Jensen, 2005).

1.2.1.1 Radiometric Correction

The measured pixel in a satellite or remotely sensed image can be affected by various artifacts which affect the recorded Digital Number (DN) in the image. Radiometric distortion can occur in two main ways i.e. "relative distribution of brightness over an image in a given band can be different to that in ground scene and/or secondly, the relative brightness of a single pixel from band to band can be distorted compared with the spectral reflectance character of the corresponding region on the ground" (Richards & Jia, 2006).

Correction for radiometric correction can be achieved by either absolute radiometric correction which is converting digital number recorded in the image pixel to top of atmosphere reflectance using band gains and offsets, solar irradiance and solar zenith angle. Therefore, absolute radiometric correction is used to approximate DN values in the image to radiance on the earth surface (Du, Teillet & Cihlar, 2002).

The other method is relative correction, which is to normalize intensities of multi-temporal imagery taken on different dates to a selected reference/standard imagery specified by the user at a specific time. The technique can also be performed using different bands within a single-date remote sensed image (Jensen, 2005). This is performed to ensure that the two images have approximately the same radiometric characteristics to each other by normalizing them to a common radiometric scale reference (Du, Teillet, & Cihlar, 2002). The technique may involve either histogram-matching between the two images to achieve relative image-to-image radiometric normalization or by the adjustment of average and standard deviation values, conversion to a normalized index such vegetation indices or the commonly used method of normalizing the two images by least square method using a linear function (Mas, 1999).

1.2.1.2 Atmospheric Correction

The most difficult task in remotely sensed data pre-processing is the correction for atmospheric effects. Most advanced remote systems processing software programs have algorithms for near perfect geometric corrections, yet there is a sluggish development and implementation of atmospheric correction models (Chavez, 1989). The fact is, there are numerous atmospheric models developed but none have been able to deliver perfect results.

There are a different number of ways to correct for atmospheric correction. These may include calculating atmospheric conditions based on physical attribute of a place such as time of the year, altitude, and coordinates of the place. Also, the atmospheric models such as LOWTRAN, MODTRAN and its derivatives (e.g. ATCOR2 and ACORN) and 5s code can be predictated using in situ data taken at the time of imagery acquisition (Jensen, 2005). Image-based methods such as Dark Object Subtraction (DOS) and Improved Dark object developed by (Chavez, 1988). “Atmospheric correction reduces the errors in estimating surfaces reflectance and can also be used to set datasets to a common radiometric scale” (Song, Woodcock, Seto, Lenney & Macomber, 2001).

Song et al. (2001) concluded that it is not necessary to perform atmospheric correction before performing change detection or classification.

1.2.1.3 Geometric Correction

Geometric errors can occur due to various sources, some of these are rotation of the earth during image acquisition, the earth's curvature, scan time skew, aspect ratio distortion and variation of platform altitude and velocity of the remote sensing systems (Richards & Jia, 2006).

When comparing changes between two remote sensing imageries acquired on different dates, it's essential to process them together. It is important to achieve pixel by pixel registration between the two images before a comparison is made (Richards & Jia, 2006).

Correcting for geometric errors can be done in two main ways and/or the combination of both. These are:

i. Image-to-map rectification is converting the geometry of an image to planimetric. However, not all topographic effects can be removed (Jensen, Introductory Digital Image Processing: A remote sensing perspective, 2005). This is achieved by simply defining a, "grid over the map to act as the grid of pixel centres in the corrected image. This grid is parallel to, or indeed could in fact be, the map coordinate grid itself, described by latitudes and longitudes, UTM coordinates and so on" (Richards & Jia, 2006).
ii. Image-to-image registration, which is registering two images so that pixel to pixel match can be made. It can also be done by registering the two individual images to a map coordinate base separately. If georeferencing is not necessary, one image can be chosen as master and the registered one as slave. Both methods involve the use of ground control points and appropriate mathematical models. The purpose of this is to remove the influence of geometry errors between the images.

Correcting for geometry requires identification of two sets of ground control points in both images and map. These ground control points should represent the same physical features in both images and/or map i.e. the base image and the referenced image. The RMS (root mean square) error i.e. geometric distortion measurement of the GCP collection should be less than or equal to 0.5 pixel. Also, GCPs collected should be uniformly distributed throughout the image to be rectified (Jensen, 2005). After the completion of this step, a chosen intensity interpolation or resampling should be applied to the rectified image.

Nearest Neighbour interpolate the pixel values of a geometrically corrected image are obtained by interpolating the brightness value closest to the original values. It is the most desired resampling method since it hardly alters the pixel brightness value during resampling. This is important when studying vegetation, water turbidity and temperature. Bilinear Interpolation assigns the output pixel values by interpolating the values of four nearest pixels to the new desired position. Cubic convolution uses a weight value of 16 input pixels surrounding the desired location to determine the output pixel value instead of 4 as in bilinear interpolation.

1.2.2 Vegetation Indices

Vegetation Indices have been extensively used to monitor vegetation dynamics since the 1960s. Jensen (2000) summarized vegetation indices as biophysical measurements that document vegetation types, productivity, and functional health needed for land resource management, tackling deforestation and promoting sustainable agriculture development. Multispectral information from different bands is used to create a single index (Green, Clark, Mumby, Edwards, & Ellis, 1998). Most of these indices are developed from the basic understanding of leaf and canopy biophysical properties. They can be used to measure the percentage of green cover, chlorophyll content and forest biomass (Jensen, 2000).

Some examples of these indices include the simplest *Simple Ratio (SR)* which is ratio of near-infrared to red band reflectance, the commonly used and generic *Normalized Difference Vegetation Index(NDVI),* and the *Soil Adjusted Vegetation*

Index (SAVI) which is an extended NDVI with a soil calibration factor to minimize background influences from soil-plant spectral interactions (Jensen, 2005; Huete, 1988).

1.2.3 Supervised Classification

Supervised classification is the commonly used method for quantitative analysis of remotely sensed data. It involves a combination of field work and analysis of maps and image using personal experience. It involves the collection of training sites using the spectral characteristic of these known areas that represent known land-cover types or classes in remotely sensed imagery. Each pixel is then assigned to a class that resembles its spectral signature defined by a user during the training phase of the process using a variety of algorithms (Jensen, 2005; Richards & Jia, 2006).

1.2.4 Unsupervised Classification

This classification technique is used when land cover types are not known to prior classification due to lack of ground reference information or when the surface features on the image are not well defined. Special algorithms in a remote sensing software package group pixels with similar spectral characteristics into distinctive classes. However, the technique requires very minimal initial input information of classes such as number of classes should be specified (Jensen, 2005; Richards & Jia, 2006).

1.2.5 Change Detection Techniques

The objective of this study is to account for sustainable land management and practices and biophysical dynamics related to changes in the land. This is where change detection techniques come in handy. Singh (1989) defined change detection as "*the process of identifying differences in the state of an object or phenomenon by observing it at different times*". Change detection can be used to monitor vegetation cover changes, urban expansions, planning and management of land (Singh, 1989). There has been a huge development of change detection methods using data from remote sensing systems to monitor and account for the changes in land dynamics

(Song, Woodcock, Seto, Lenney, & Macomber, 2001; Mas, 1999; Singh, 1989). Changes in land covers include determining intensity and rate of the change also, whether certain variable contributes to the change or not (Jensen, 2005).

It is essential to pre-process the images before performing change detection. These steps include, accurate spatial registration, radiometric correction, atmospheric and correction for topographic effects in the mountainous areas (Lu, Mausel, Brondizio, & Moran, 2004; Singh, 1989). The following are the most common methods used for change detection for identifying environmental changes.

1.2.5.1 Image Differencing

The technique involves calculating the difference between two images obtained on different dates by arithmetically subtracting the pixel values to get a new image. The resulted image can be assigned a certain threshold to determine whether a change has taken place or not. This method is simple and provides an easy way to interpret the results. It is also a very common change detection algorithm. The technique only works for registered images.

$$I_d(x,y) = I_1(x,y) - I_2(x,y) \tag{1.1}$$

I_1 and I_2 donate the images obtained from time t_1 and time t_2, *(x, y)* are the coordinates of the pixels. The resulting image, I_d, represents the intensity difference of I_1 from I_2.

1.2.5.2 Image Ratioing

This is another method to compare images by pixel. The technique involves dividing two images from different dates pixel by pixel. It is essential to register the images before performing this operation.

$$I_r(x,y) = \frac{I_1(x,y)}{I_2(x,y)} \tag{1.2}$$

In the resultant image, unchanged pixels have a value equal to or very close to 1. If the ration is less than or greater than 1 then changes have occurred. The technique is also used for shadow, topography impacts and sun angle correction

1.2.5.3 Image Regression

The method is the assumption that pixels of one image I_2 are a linear function of pixels of another image I_1. So, the brightness values of the second image (reference) can be regressed against those of the other image (subject) using least-squares regression.

$$\hat{I}_2(x,y) = aI_1(x,y) + b \tag{1.3}$$

The squared error is defined between measured data and predicted data to estimate the values of *a* and *b*. This technique is useful to reduce the effects of atmospheric conditions

1.2.5.4 Vegetation Index Differencing

This is the use of vegetation index for calculating image difference. For example, Normalized Difference Vegetation Index (NDVI) is widely used to monitor vegetation dynamics, but can be extended by computing the difference of two images obtained on different dates. The requirement is that the original images used to derive the NDVI should be atmospherically corrected (Jensen, 2005).

$$\Delta NDVIij = NDVIij\,(1) - NDVIij\,(2) \tag{1.4}$$

Where *ΔNDVIij* = change in NDVI value, *NDVIij* = NDVI (1) value on Date 1 and *NDVIij* (2) = NDVI value on Date 2.

1.2.5.5 Post-Classification Comparison

This is the quantitative and widely used technique for change detection (Song, Woodcock, Seto, Lenney, & Macomber, 2001). It requires a comparison of two independently classified images from different dates. The images are first rectified and thematic maps are produced from them. The resultant two maps are then compared on pixel-by-pixel basis (Jensen, 2005). Errors in individual classified images will affect the final results accuracy (Lu, Mausel, Brondizio & Moran, 2004).

Post-classification comparison provides the advantage of "from-to" change class information (Lu, Mausel, Brondizio, & Moran, 2004). In this method, the need to perform geometric and atmospheric corrections is removed (Lu, Mausel, Brondizio, & Moran, 2004; Singh, 1989). Mas (1999), obtained the highest accuracy using the post-classification comparison based on supervised classification of two images.

1.2.5.6 Principal Component Analysis (PCA)

The principal components are based on the eigenvectors of the variance – covariance matrix of the merged data set. PCA is used to reduce the number of spectral components to fewer principal components accounting for the variance in the original multispectral satellite images (Singh, 1989). The PCA of images collected from different dates can be differenced to calculate for the change detection between the images. The disadvantage is that the method is difficult to interpret change information in the resultant image.

1.3 Climate Change

Climate change refers to any substantial change in measures of climate (such as temperature or precipitation) lasting for an extended period (decades or longer). Climate change may result from natural factors and processes or from human activities (EPA, 2014).

1.3.1 Climate Change Causes

The existence of life depends hugely on the energy that comes from the sun, about half of light energy is absorbed by the earth and then radiate back in the form of infrared heat. Approximately 90 percent of this heat is absorbed by greenhouse gases molecules (such as carbon dioxide, nitrous oxide, water vapour and methane) and radiated back to warm the surface and lower atmosphere to a life-supporting average of 15^0 C.

1.3.1.1 Tectonic Plates

In 1915, a scientist called Alfred Wegener, for the first time hypothesized a continental drift theory. According to this hypothesis, 165 million years ago the earth did not have 7 continents; all the continents were just a huge mass of land called Pangaea. The ocean surrounding this land mass was called Panthalassa. The movement of plates caused this huge mass of land to be separated into two parts which formed the northern part called Laurasia and the southern parts was known as Gondwanaland. These two continents were separated by an ocean called Tethys. With the movement of the layers the continents were well separated to their present state and 7 continents started to take shape. In Figure 1.1 the movements of the continents from Pangea are illustrated.

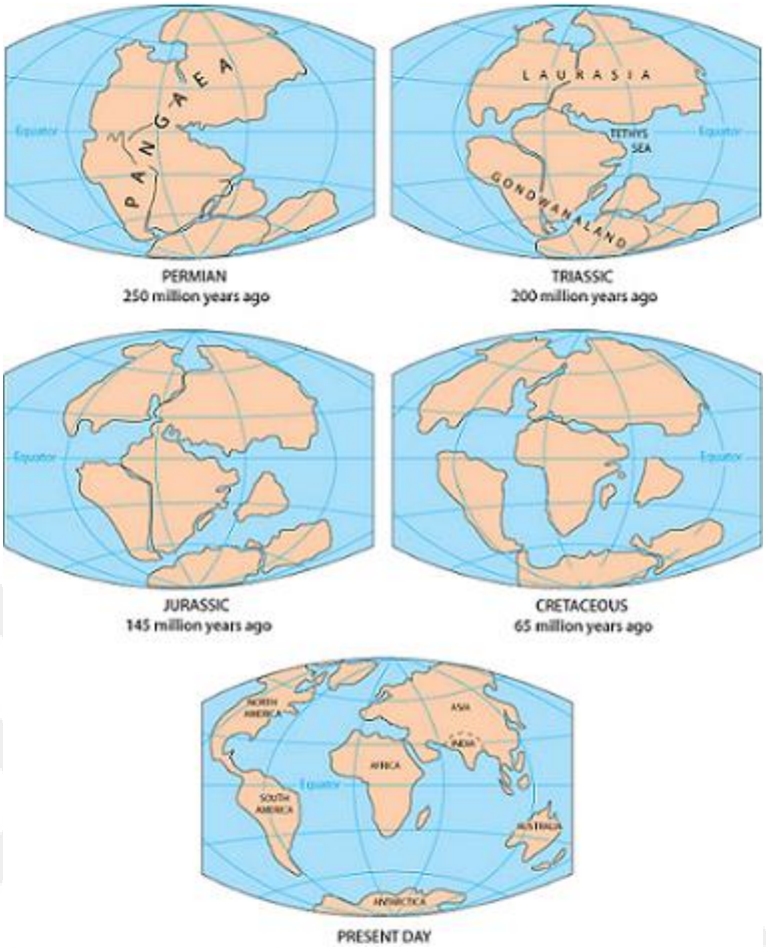

Figure 1.1 From Pangea to the present (United State Geological Survey, 2012)

In geological terms, the mentioned tectonic plate theory is one of the theories that provides an explanation for the great ice age period. Naturally, glaciations can only occur on land. These glaciations took place in the old earth in area areas with high latitudes. Many people in the world of science, it indicates that when the ice age occurred the continents moved from tropical latitudes towards the poles.

The results of present research, have found ice caps in unexpected locations. These areas are India, Africa, South America and Australia. These areas in tropic and subtropical regions went through a period called late Palaeozoic ice age that took place around 250 million years ago. However, no traces of glaciations were found in the high latitudes of North America and Europe. This is an astounding question that requires an answer. This surprising situation can only be answered best by using the tectonic plate theory.

The above-mentioned ice continents that were formed during Pangea remain as current ice caps as seen today. It is known that India, Africa South America and Australia were in the southern high latitudes of their current locations. Through time the continents separated and these plates moved to the different regions they are found today. This situation is explained in Figure 1.2 (below). In the first figure, the areas in white, show the areas that were covered by ice in the Pangea continent approximately 300 million years ago. The second figure shows the continents in their present state. White areas show the areas that were covered by ice caps.

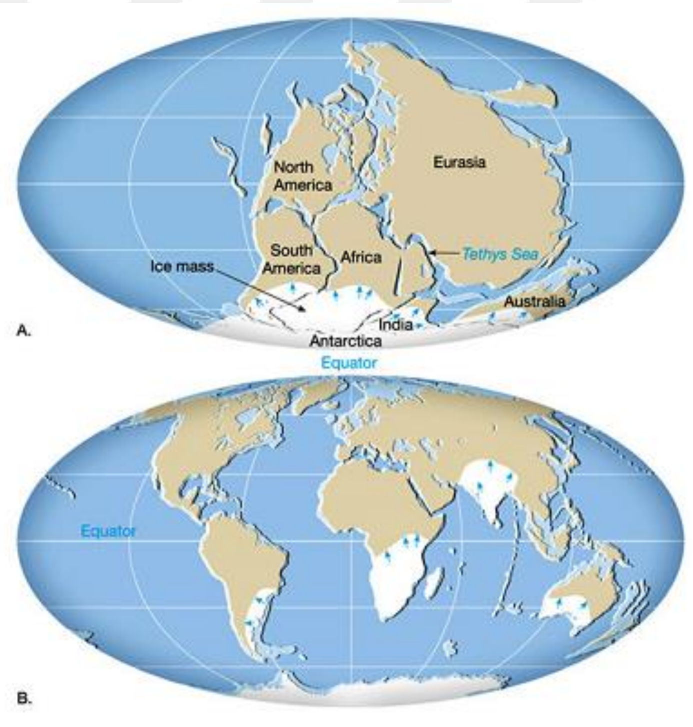

Figure 1.2 A) The areas covered by glacial ice in Pangea B) The present location of the continents (Cosscience1, 2010)

Of course, these continental movements did not take place in one day or a few weeks. These movements took place extremely slowly over a large geological time period. These periods took effect millions of years ago. The desertification of Tibet is a good example of this. Forty million years ago the Indian plate and Tibet plate crashed into each other resulting in the formation of the Himalayan Mountains. The Himalayan Mountains blocked the rainy clouds from the sea and the Tibet that once was full of fauna and flora turned into a desert. This movement was only a few centimetres per year. In addition to this slow progress changes in ocean circulations: transforming into heat and humidity contributed to climate changes.

1.3.1.2 Volcanism and Meteors

The opinion that volcanism could cause climatic changes was put forth many years ago. The spread of materials created as a result of volcanic eruptions causes the release of a huge amount of gases and fine grains of ashes. Figure 1.3, illustrates this situation in Mt. Etna volcano eruption in October 2002 on the island of Sicily. Mount Etna is the largest and most active volcano in Europe. One of the released gases, known as thermostat gas, is sulphur, which composes 70% of the gases in volcanic eruptions.

The task of sulphur is to reflects solar energy from the sun and carry away the reflected energy from the earth to the atmosphere. Carbon dioxide (CO_2), which is a greenhouse gas, is responsible for the increase of earth temperature and it does this by forwarding the solar energy from the sun to the earth and blocks the reflected energy from the earth to the atmosphere. In short, in normal circumstances when the CO_2 content in the atmosphere increases sulphur steps in and as a natural process and reduces the temperature.

Figure 1.3 The explosion of Mount Etna as seen from the space (NASA, 2010)

The huge volcanic eruptions release enormous amounts of gas and ash that can reach very high into the atmosphere. Due to currents in the atmosphere, these gases and ashes are spread all around the earth and can be suspended in the atmosphere for a number of months or years. The suspended volcanic materials block the emitted energy from the sun from reaching earth. An example to explain this phenomenon was given by Benjamin Franklin concerning an event that took place from 1783 – 1784. At this time, it was hypothesized that Iceland passed through a period of extreme cold winters that could have resulted by the release of materials from volcanic eruptions. Below are examples of the correspondence of volcanic eruptions and cold periods.

1.3.1.2.1 Tombora Volcano. Tombora Volcano is located in Indonesia on Sumbawa northern coast. The volcano is not active at present but between 7 – 14 April in 1815 it erupted and as a result of this explosion a total of 92,000 people were killed. Of these 92,000 people, 11, 000 to 12,000 died during the eruption and the remaining died afterwards due to famine and diseases. The explosion reached a height of 3,900 metres and the result was around 100 km^3 of ash being violently released. After this explosion, the year 1816 was known as the year without winter (Ramirez, 2012).

Especially during the months of May to September, the northern east of the United States and some areas of Canada experienced severely cold weather that was never experienced before. The seasons were reversed. Normally, in the month of June when the hot weather was expected a heavy snow fell and between July – August they experienced frost. The earth witnessed a recorded drop of global rainfall by between 3.6% and 4% in 1816. According to tree circles, the summer of 1816 was colder than 1815 by 1.5 °C (Ramirez, 2012).

1.3.1.2.2 El Chichon Volcano. El Chichon Volcano is located inside the borders of Mexico. It erupted in 1982, and it was one of the most tracked eruptions in the world of science. The results of the investigations conducted confirmed that this explosion reduced the global temperature by 0.3 – 0.5 °C. The eruption of this volcano was smaller when compared to that of St. Helens in Washington State in the United States. However, one question comes to mind, “Despite the eruption being smaller why did it cause global cooling?” The answer to this question was found from the results of the experiments conducted and the answer was in the materials spread by this explosion.

The released materials from the Mt. St. Helens eruption were mainly ashes that took a very short period of time to fall. The materials released from El Chichon eruption were estimated to contain 40 times more sulphur dioxide than those released by the Mt. St. Helens eruption. The typical characteristics of sulphur dioxide is if it reaches the stratosphere and if it contains water vapour, it forms a huge cloud composed of very small particles of sulphuric acid. It takes a number of years for these particles to dissipate completely (Robock, 2002).

In this situation the light coming from the sun failed to reach the earth, therefore temperatures dropped. In Figure 1.4, shows the changes in measured solar radiation from 1970 - 2003 by Hawaii's Mauna Loa Observatory. Figure 1.4 shows changes in solar radiation that reached the surface of the earth after the eruptions of El Chichon and Pinatubo.

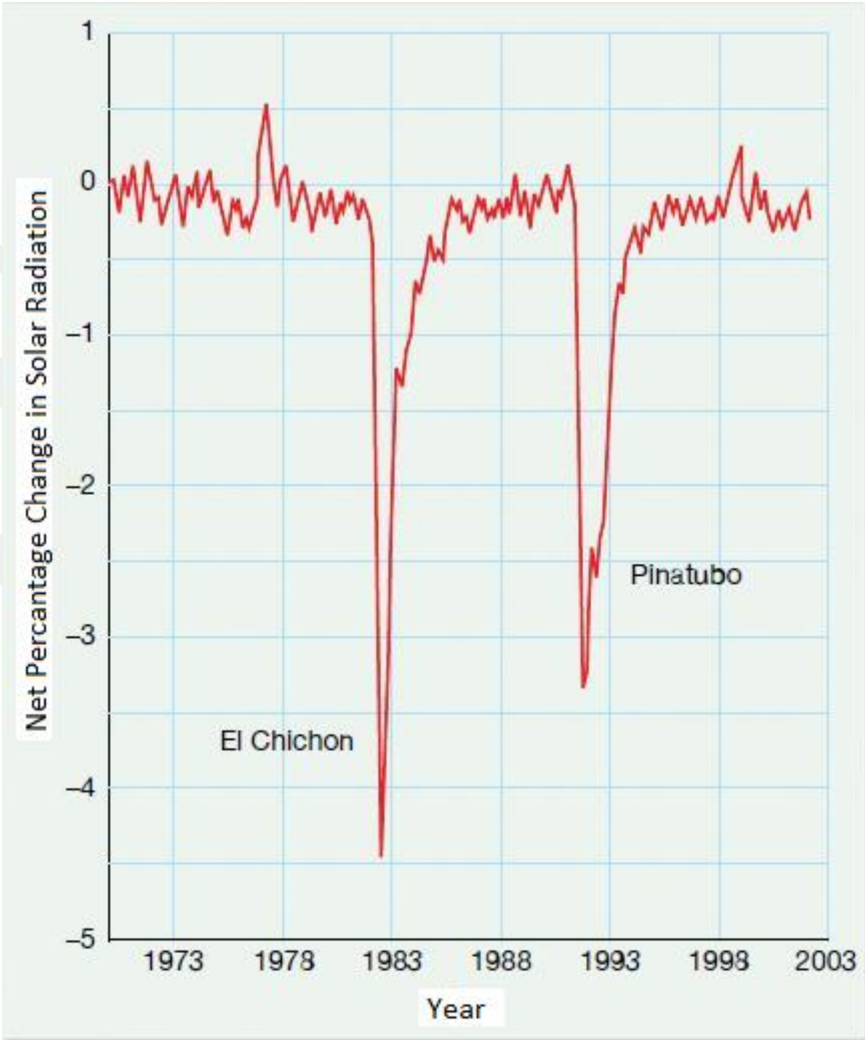

Figure 1.4 Changes in solar radiation and the effect of the volcanos between 1970 - 2003 (Space Systems Research Laboratory, 2005)

As a result of these investigations it is seen that after the volcanic eruptions the clouds that stayed in the atmosphere for many years were not composed of dust but they were made of sulphuric acid.

1.3.1.2.3 Pinatubo Volcano. Pinatubo Volcanic eruption occurred in the Philippines, on the island of Luzon. This volcanic eruption took place in June of 1991 and was one of the most violent volcanic eruptions of the 20th century. The ash cloud from this climactic eruption ascended 35 km into the air. The year following the eruption saw a decrease of global temperature by 0.5 °C which was caused by the released aerosols into the stratosphere (nearly 20 million tons of sulphur dioxide) and a very serious decrease in rainfalls (Newhall, Hendley & Stauffer, 1997).

Despite the Pinatubo volcanic eruption being one of the largest volcanic eruptions in the 20th century the earth has volcanoes 400 times larger than this. The results of such huge explosions could cause a nuclear winter lasting for 6 to 7 years.

If we look at meteors, their effects are similar to those created by volcanoes on the earth. Depending on the size of the meteor the created dust that reaches the atmosphere could block the light rays from the sun reaching the earth and causing global temperatures to decrease. An example of this can be given by the extinction of the dinosaurs that lived on the earth millions of years ago.

Meteors that struck the earth 66 million years ago are believed to be a reason for the extinction of the dinosaurs. Another point of view is that the disappearance of the dinosaurs was caused by very violent volcanic eruptions. Whether it was meteors or volcanism, the result was the earth experienced some very cold temperatures, food was scarce and the result was the extinction of those creatures that were at the top of the food chain in a very short period of time, which were the dinosaurs.

1.3.1.3 Solar Energy Fluctuation

In this section, solar energy fluctuations, their results and sunspot cycles and the coming cycles will be examined. A reason for changes in solar energy can be found in two basic ways. The first one is, the sun being a star: is the results of changes in its core. The second one is, in the convection regions of the sun and its magnetic areas.

1.3.1.3.1 The Sun. The surface temperature of the sun is around 5,800 K and the core temperature can reach up to 15,600,000 K. The energy released from the sun takes 8.44 minutes to reach Earth from the surface of the Sun (Williams, 2016). The sun which is in the state of plasma, create its energy at its centre. Creation of this energy involves a nuclear fusion reaction that happens by converting hydrogen into helium. This reaction only takes place in the centre region of the sun and the created energy is carried away from the core to the outer layers of the sun. The last layer this energy reaches is called the photosphere. From this point onwards it is spread as sunshine and solar energy particles into space (Shlionskaya, 2011). In Figure 1.5 (below), is an image of the sun.

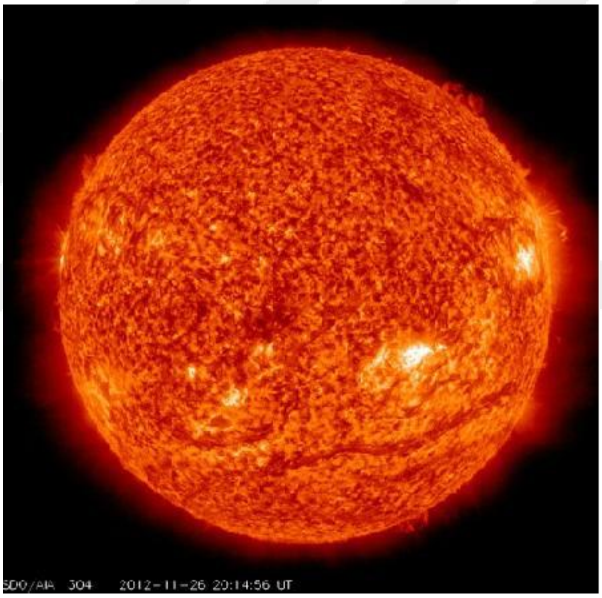

Figure 1.5 The Sun (NASA, 2012)

Since the sun has extremely high temperatures, its contents are found in either gas or plasma state. This results in a rotational movement known as differential rotation. This means the regions near the equator move faster than those at the poles. A rotational movement around the equator is 25 days while at the poles is 35 days. The result of this is the creation of nonlinearity magnetic lines and formation of magnetic regions. These magnetic rings explode from the solar surface and create solar eruptions and sunspots.

1.3.1.3.2 Sunspots. The effects of the spots formed on the surface of the sun have been known for more than 2000 years. With varying size, the largest ones can reach a diameter of 50,000 km. With such enormous size, they can be visible to the naked eye. On average their size can be the size of the earth. Temperatures in these spots, seen as dark areas on the surface of the sun, can reach lower levels of more than 500 K (Shlionskaya, 2011). Figure 1.6 and Figure 1.7 show example of these spots

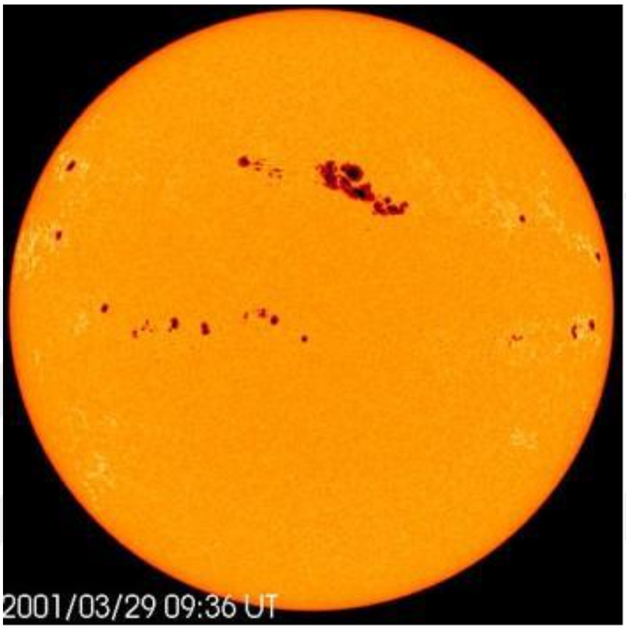

Figure 1.6 Sunspots (European Space Agency, 2001)

A typical sunspot consists of a dark central region called the umbra and light coloured surrounding outer section known as the penumbra. If an average sunspot is cut out of the Sun and placed in the sky at night, it would be as bright as a full moon. The centre regions of the umbra are the areas with highest magnetic values. The meaning of the darkness of these areas is that they are caused by magnetic cooling. The temperatures in these spots are around 3,800 K. These spots showing areas with high magnetic field formation are usually found in groups and they are seen to last between a few hours or a few months. The spots can be seen due to the rotation of the sun on its axis from east to west.

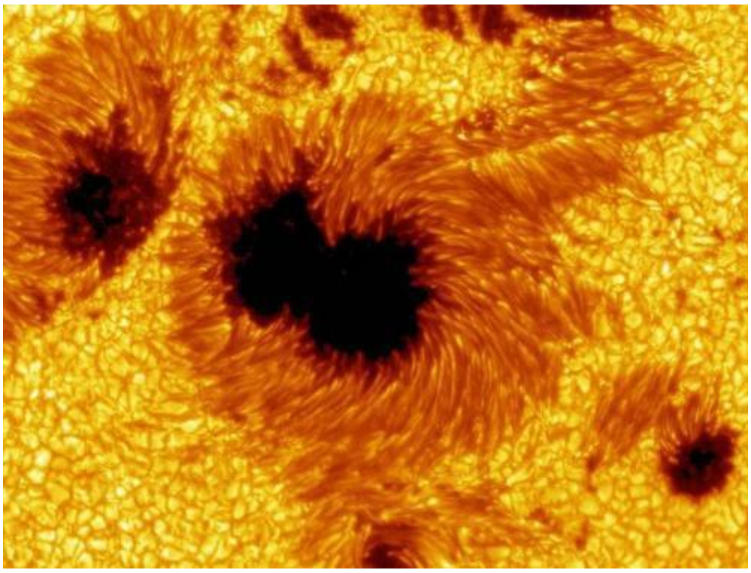

Figure 1.7 Sunspots (ESA, 2013)

The increase and decrease of these spots over time give information and clues about the solar activity. If magnetic activities of the sun increase, the result is increased the formation of sunspots. With the increase of solar activity, the magnetic fields loop convection layer surpasses the photosphere and are released outside. It creates magnetic flux loops emerging from the regions of the sunspot. These loops are thrown from the surface of the sun and reach a height of 300-500 thousand kilometres. For easy understanding of this magnetism, a magnet was placed in the spot region in Figure 1.8 (below). When watched from the earth the circulation of solar surface with sunspots takes 27 days to complete. The more complicated the structure of the magnetic field the higher the chance of producing explosions. Figure 1.9 (below) shows a flare created in the solar explosion.

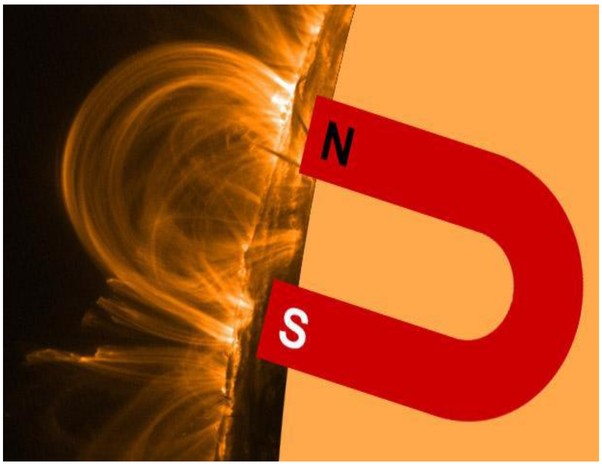

Figure 1.8 Sunspots magnetism (NASA, 2012)

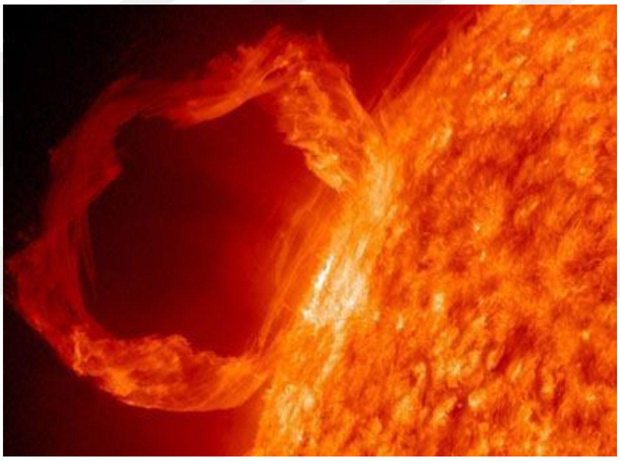

Figure 1.9 Flare explosion in the Sun (NASA, 2014)

1.3.1.3.3 Sunspot Cycle. There are several periods consisting of increases and decreases in the number of sunspots. From these periods the minimum lasts for an average of 11 (9-13) years. When this cycle starts the number of sunspots is at a minimum and it increases as time goes by and when the cycle reaches the middle the number of sunspots reaches the maximum level (Williams, 2016). At the end of the cycle, the number of the sunspots decreases to the minimum levels. Figure 1.10 (below) illustrates the sunspot cycle.

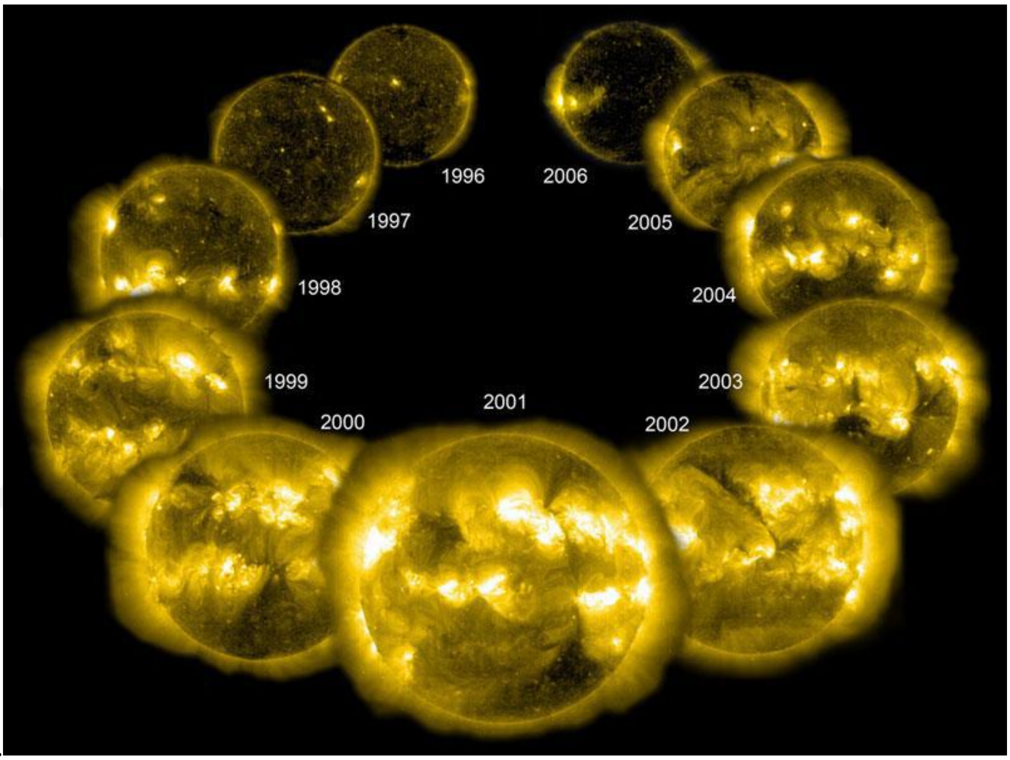

Figure 1.10 A typical sunspot cycle (NASA, 2012)

The sunspots could be explained using a “butterfly diagram”. The diagram shows the areas where the sunspots are formed. Sunspots are formed both in northern regions and southern regions (Figure 1.11).

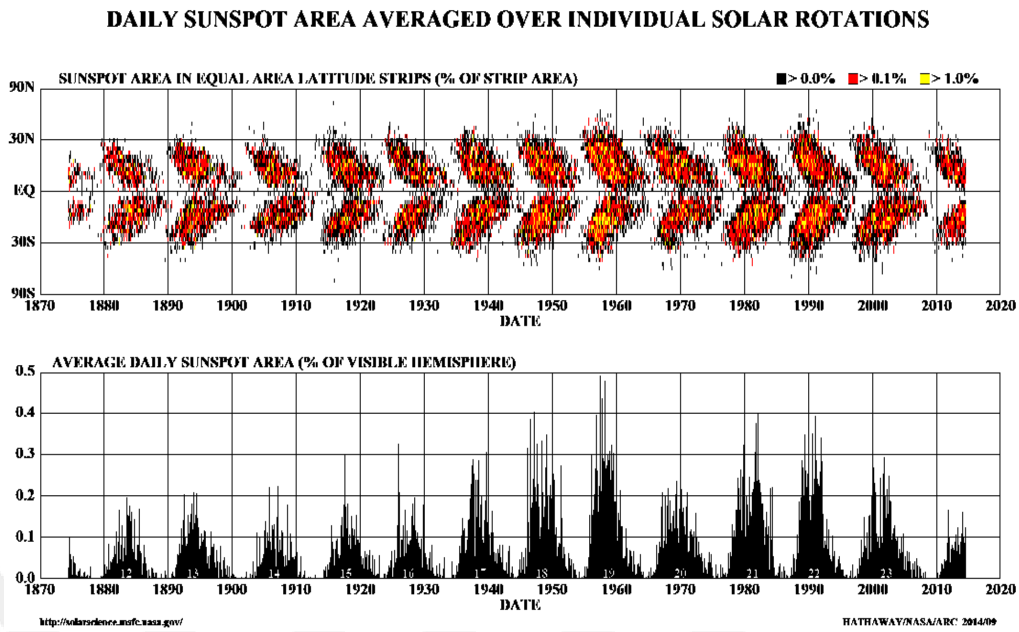

Figure 1.11 Butterfly diagram showing paired Spörer's law behavior (NASA, 2016)

The 11-year sunspot that forms on the basis of three principles. The first principle is Schwabe-Wolf principle. In the 11-year sunspot cycle changes in the sun and emissions takes place in the same margin/frameworks. The events in the cycle take place so fast and have a straight tendency in the middle.

This explains that the value of slope at the beginning of the cycle have higher values than the values of the slope at the end of the cycle. The result of this is the maximum values do not happen in the middle but rather near the starting point. The second one is Spörer’s Law, which according to this law, the sunspots within 11- year cycle appear first at high heliographic latitudes; during the course of the cycle, the mean latitude of sunspots gradually decreases (Roschina & Sarychev, 2010). The spots in every cycle are formed in both hemispheres at around 40 degrees’ latitude. With the passage of time, the spots gradually descend to lower latitudes of around 5 degrees and become visible. The result of this principle is Hale principle. When the next cycle occurs the magnetic polarities return the opposite way in each hemisphere.

At the beginning of the cycle, very few sunspots are seen or sometimes they cannot be seen at all. This is a normal situation. As time increases, as explained by Spörer law, the number of sunspots increases and they move straight to the equatorial region. The sunspots usually occur in pairs and each one has an opposite magnetic pole. On average, these magnetic poles change every 11 years. When the poles return to their starting points, they complete a full magnetic cycle and this cycle takes 22 years. Since this process has a dynamic structure, the cycle period also experiences changes.

It is understood that when the sunspots reach their maximum size plants grow up very fast. The number of sunspots has an interaction with wheat price. When the number of sunspots is low the price of wheat increases. That means, when sunspots are few, less wheat is grown and as a result the price increases (Herschel, 1801).

1.3.1.3.4 Correlation between Solar Energy and Temperatures. The energy from the sun that reaches the atmosphere of earth is called a solar constant. On average this energy has a value of 2.00 Cal/cm^2/min. According to measurements conducted this value is not constant but it fluctuates from time to time (Oliver J. and Fairbridge R., 1987). When a number of sunspots and solar activity decreases this value also decreases to around 1.92 Cal/cm^2/min, and when the sunspots number and solar activity increases the value shows an increase to approximately 2.04 Cal/cm^2/min. These changes also affect climate change in the long term. Changes in the solar constant have a direct relationship with solar activity. When this value decreases to 1.96 earth experiences long term cold climate, and when it increases to 2.04 a hot climate is experienced. Figure 1.12 is taken from research done by Rohde (2006) demonstrating the relationship between solar radiation reaching the earth and the sunspots.

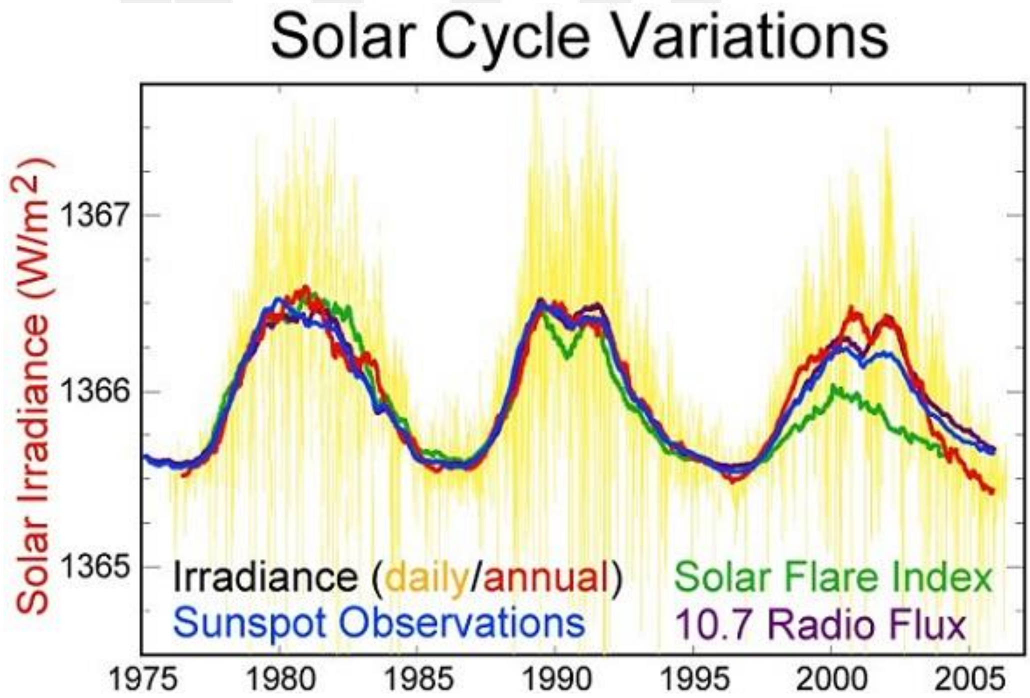

Figure 1.12 Changes in radiation from the Sun (Rohde, 2006)

1.3.1.4 Human Activities

Scientists all over the world agree that the current trend is climate change is from human activities. Over the last centuries, use of fossil fuels, such as, coal and oil have led to an increase in carbon dioxide concentrations in the atmosphere which in turn has led to the expansion of the greenhouse effect. This is coupled with the clearing of land for agriculture and other human activities that increase greenhouse gases in the atmosphere (NASA's Jet Propulsion Laboratory, 2016).

Human activities that depend on industrial development have contributed directly to raising of atmospheric carbon dioxide levels from 280 parts per million to 400 parts per million over the past 150 years (IPCC, 2007).

1.3.2 Climate Change Indicators

The climate is changing and to track these changes scientists use some indicators as reference measurements to establish that the climate is really changing. Most of these indicators suggest that there is correlation between the changing of climate and human-induced greenhouse gases emissions.

1.3.2.1 Air Temperature over Land and Sea Surfaces and Global Precipitation

Temperature measurement is one of the ways to detect an overall change of climate. Temperature measurements are collected from weather stations on land. With the advancement of satellite technology, it is possible to estimate the earth’s temperatures using imagery collected from satellite data. This has enabled the collection of highly precise temperature data collection since 1979.

Measurements of low and high temperatures, frequency of heat waves and anomalies in summer and winter temperatures are used as indicators for climate change (EPA, 2014). For instance, data noted overall warmer temperatures than average in eastern Africa during 2009.

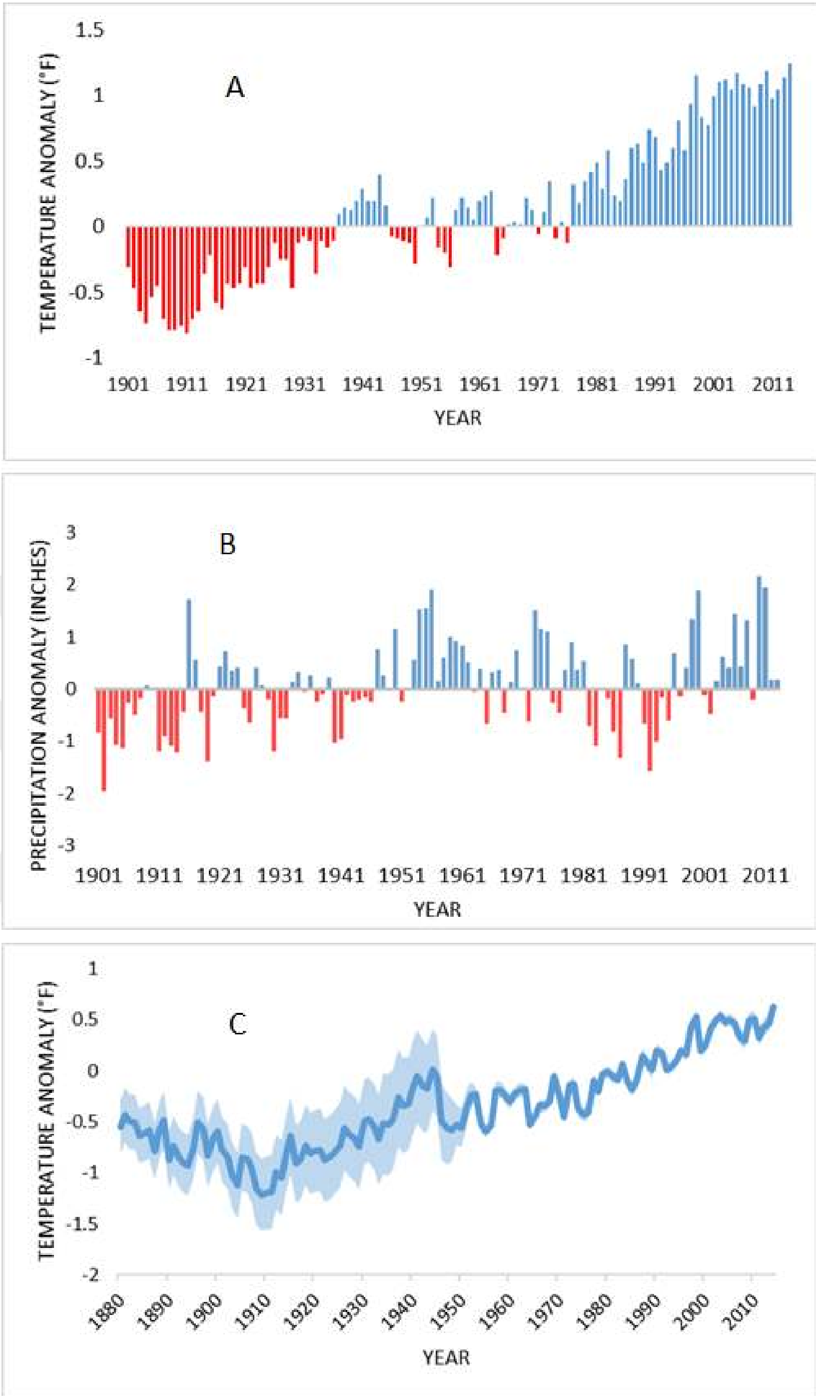

Figure 1.13 Climate change indicators, A) Earth's surface temperature anomaly B) Global precipitation anomaly C) Average global sea surface temperature anomaly

1.3.2.2 Heat Trapping Gases

Since the mid-20th century, the globe has witnessed an increase of concentration of greenhouse gases in the atmosphere especially through human activities. The build-up of these gases in the atmosphere leads to the increase of global temperature. The indicator measures carbon dioxide, methane, nitrous oxide, and several fluorinated gases emissions (EPA, 2014). Even if we stop all human emissions another increase of 0.5 F is expected to raise in the few coming decades. This is due to the past and existing greenhouse gases effect, which will also affect the future global warming (Walsh et al., 2014).

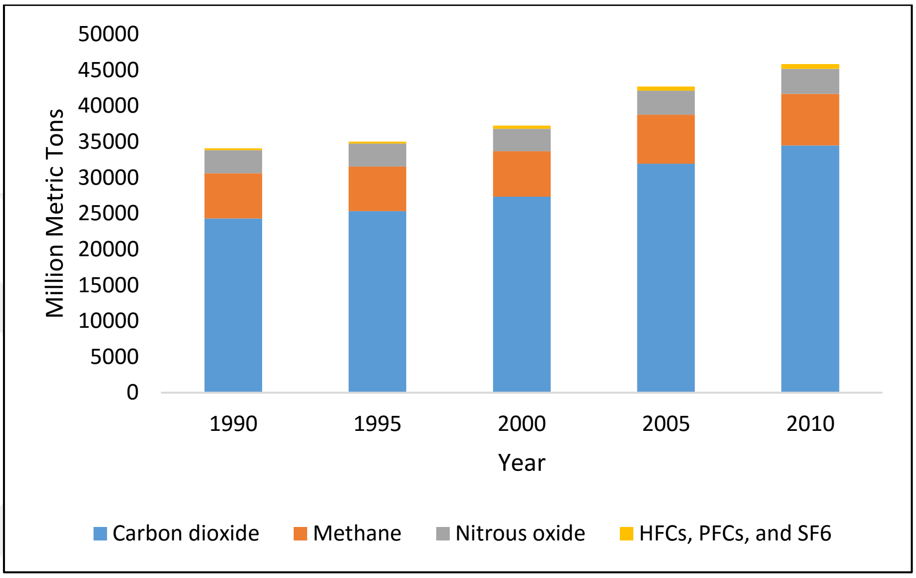

Figure 1.14 Worldwide emissions of carbon dioxide, methane, nitrous oxide, and several fluorinated gases from 1990 to 2010 (WRI, 2014; FAO, 2014)

1.3.2.3 Arctic Sea Level

Evidence suggests that there is a decrease in Artic ice extent, warming and an increase acidification of Artic Sea. This will affect the ecosystems and organisms in Arctic Sea.

The indicator measured an increase of up to 5° C in temperature in the Arctic sea, even "surface air temperatures in the Arctic have warmed at approximately twice the global rate". Minimum ice extents in a year usually occur in the month of September but data shows an overall decrease of ice extent in the Arctic Sea in all months.

The extent of the ice can be also affected by other factors including fluctuations in oceanic and atmospheric circulation (EPA, 2014).

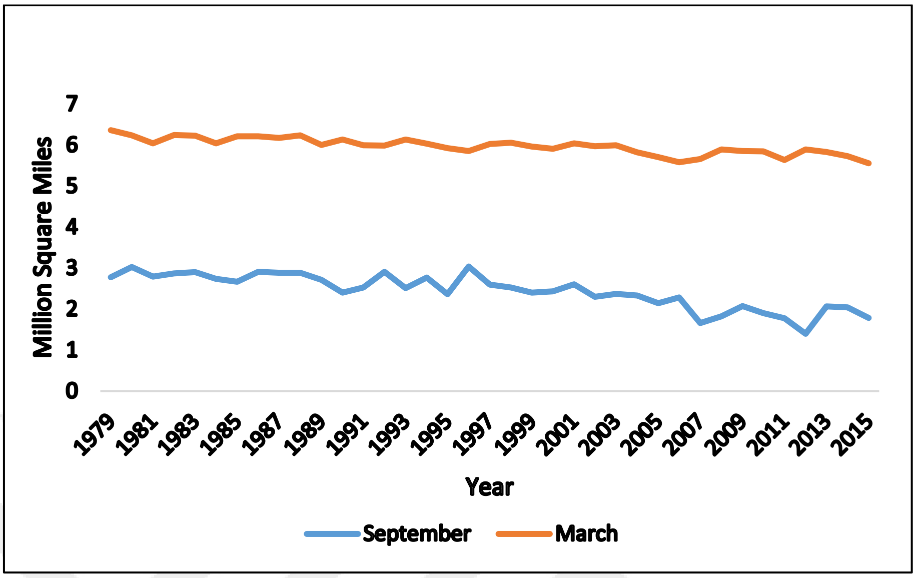

Figure 1.15 Arctic sea ice extent for the months of September and March of each year from 1979 to September 2015 and March 2016 (NSIDC, 2016)

1.3.2.4 Ocean Heat

Oceans act as a reservoir for heat in our climate system (Doney et al., 2014). However, the stored amount of heat absorbed from sunlight energy in the oceans has increased substantially since the middle of the past century. Ocean heat-effect the sea surface temperature, water circulation and sea level due to thermal expansion, which in turn have an effect on climate. High concentration of greenhouse gases causes more energy to be trapped. Despite absorbing more heat energy from the sun than the atmosphere, it takes centuries for oceans to warm compare to the atmosphere (EPA, 2014).

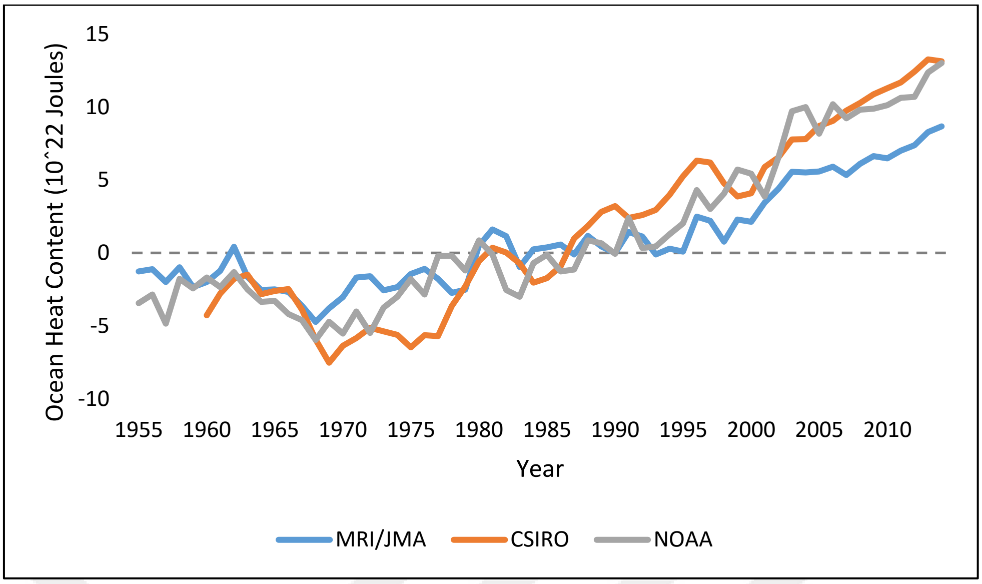

Figure 1.16 Changes in ocean heat content between 1955 and 2014 (CSIRO, 2015; MRI/JMA, 2015; NOAA, 2015)

1.3.2.5 Snow, Glaciers and Ice Sheet

The ice and snow on our planet are in the form of frozen lakes, rivers, snow covers, and ice sheets. Change in the coverage and quantity of this ice can be directly linked to the change of our climate as snow and ice are converted into water that is filling up oceans and other water bodies. The indicator measures the percentage of precipitation recorded in the form of snow from weather stations. That is the height of accumulated snow in a given day.

Recorded measurements of glaciers mass can also be seen to be decreasing at an alarming rate since the 1970s, and even this rate has accelerated in the last decade.

The availability of snow cover data from satellite sources can be tracked from the middle of the past century, as prior to that no enough evidence of ice cover changes is available.

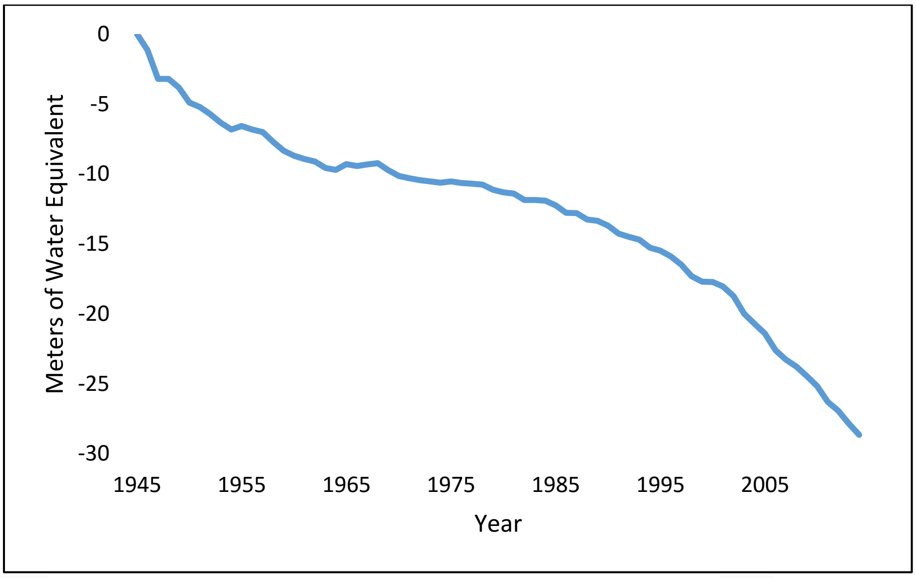

Figure 1.17 The cumulative change in mass balance of a set of "reference" glaciers worldwide beginning in 1945 (WGMS, 2015)

1.3.2.6 Sea Level

The increase of the sea level is due to the thermal expansion of water due to an increase of heat content of the ocean. The changes of water in oceans is also due to the changes of water in glaciers and ice sheets on land. Melting glaciers in polar regions with the aid of shifting winds increase the volume of water in the oceans, hence the increase of sea level.

Sea level changes occur in two ways, “Relative sea level change is how the height of the ocean rises or falls relative to the land at a particular location”. On the other hand, “absolute sea level change refers to the height of the ocean surface above the centre of the earth, without regard to whether the nearby land is rising or falling”. There is an accelerated increase of average sea level globally, with the average increase of 0.06 inches yearly (EPA, 2014).

Water level measurements in the oceans can be tracked to the late 1700s using tide gauges, while the development of satellite systems has enabled the use of satellite altimetry to measure ocean water levels with a high-precision since 1992 (Stocker et al., 2013). Between 1993 and 2012 an increased sea level rise of 3.2 mm per year was measured using satellite altimetry technology (IPCC, 2013).

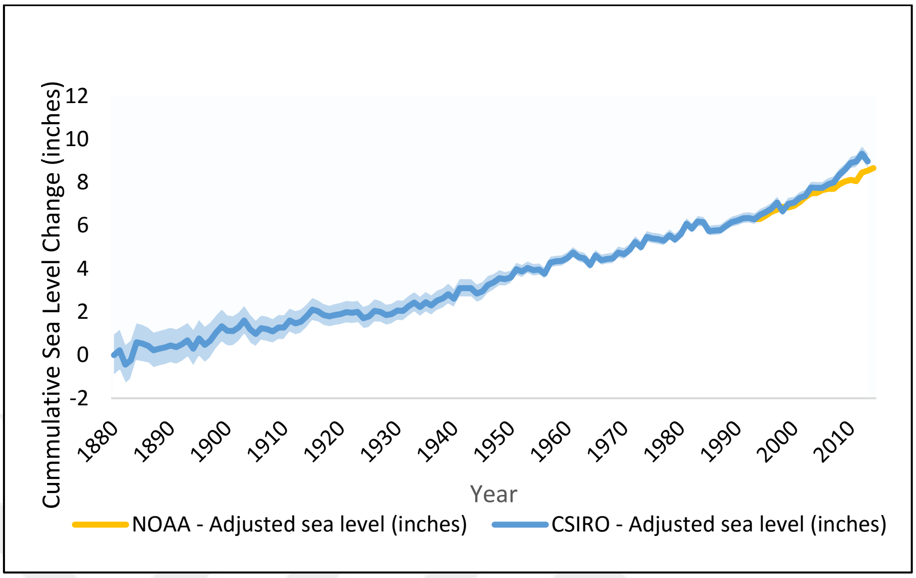

Figure 1.18 Cumulative changes in sea level for the world's oceans since 1880 (CSIRO, 2015; NOAA, 2015)

1.3.2.7 Ocean Acidification

Oceans have a significant role in monitoring carbon dioxide in the atmosphere. However, due to an increase in carbon dioxide levels in the atmosphere, oceans have to absorb more carbon dioxide, as atmospheric carbon dioxide has risen by almost 40% beyond pre-industrial levels (Doney et al., 2014). This releases extra carbon dioxide from the atmosphere which in turn has a negative effect on the ocean ecosystems, since the dissolved carbon dioxide reduces the pH levels of the oceans (EPA, 2014). The ocean acidification can also be caused by changes of other chemicals from volcanic activities release of nitrogen and sulphur compounds.

The indicator assesses the pH trend in surface water in the oceans from observations and models made in some selected stations (Stocker et al., 2013), since it can take up to centuries for pH to change in deeper water (EPA, 2014).

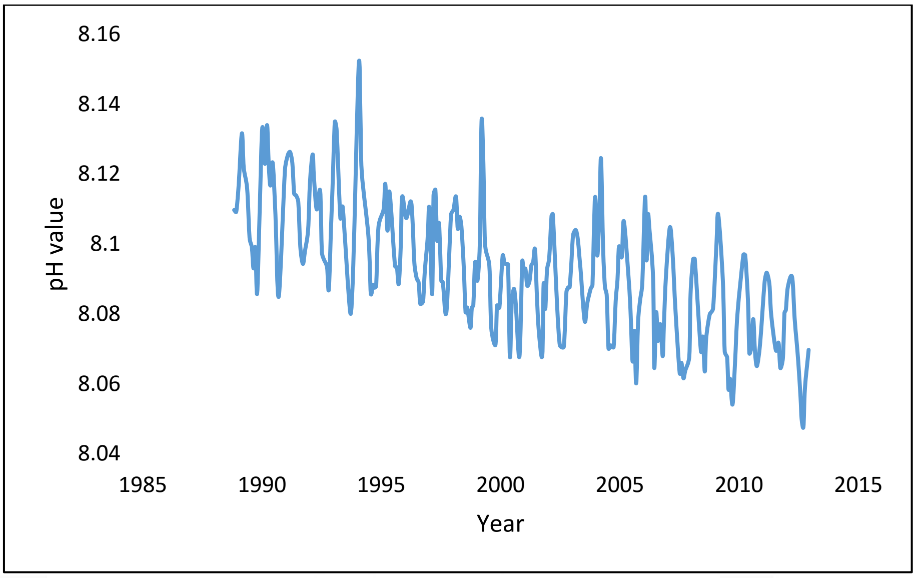

Figure 1.19 Changes in ocean acidity. The data come from observation station in Hawaii (Hawaii Ocean Time-series, 2009)

1.3.3 Climate Change Impact

The changing climate impacts society and ecosystems in a wide-ranging number of ways. For instance, climate change can affect rainfall, impact agricultural crop harvests, affect human health, and change local ecosystems. Even energy sectors can also be affected by climate change. The estimates are around 2.8 billion people are dwelling in areas prone to the negative effects of climate. These might include areas prone to sea level rises, drought, floods and intense storms (Food and Agriculture Organization [FAO], 2005).

1.3.3.1 Water

It is also essential to note that water availability is directly affected by climate change. Excessive increase in temperatures mean drought and drying of surface water (Confalonieri et al., 2007). Water is essential for ecosystems sustainability as well as for humans. Humans use water for drinking, domestic uses, agriculture and even power production.

These water uses and challenge from climate change increase pressure on water resources. In some areas, there will be a decrease of runoff and drought hence increase water demand. However, there will be floods in other areas and sea level rise and this will affect the quality of water due to contamination (EPA, 2014).

1.3.3.2 Health

Climate and weather changes have an effect on overall human health. Human health is essential in sustainable development. Changes in ecosystems, water quality and air quality affect human health. Noticed climate change effects on human health have increased heat-wave deaths, an increase of pollen allergies and distribution of infectious diseases vectors. Damaged properties from effects of storms, wind, floods and sea level rises have also effect on human psychological wellbeing. Some diseases also tend to spread when there are changes in temperatures and rainfall conditions (EPA, 2014).

Changes in the amount of rainfall and surface water can have a direct correlation with the increase of water-related diseases. Water quality and availability can be linked to diarrhoea and changes of water temperatures can have an effect on water microorganism and chemical contamination (Confalonieri et al., 2007).

1.3.3.3 Agriculture

Extreme events such as floods and drought and extreme temperatures caused by climate change have affected crop production, with farmers experiencing high temperatures and erratic behaviours in rainfall patterns and seasons (Mbilinyi, Saibul & Kazi, 2013).

Agriculture is one of the important sectors in developing countries such as Zanzibar. Around 49% percent of Zanzibaris engaged in agricultural farming in 2011/2012 agricultural year (Office of Chief Government Statistician, 2014). The dependency on agriculture is not just the case for developing countries. In addition to providing the population with food, the crops, livestock, and seafood agriculture in the United States for example, contribute at least $200 billion to the economy each year (EPA, 2014).

The conditions for optimal growth are directly dependent on the climate of as place. Temperatures and carbon dioxide concentrations can be used for growth of certain crops in some places. However, rapid and erratic changes of climate conditions pose serious challenges to farmers. Changes in overall climate conditions do not only affect the growth of crops, as animal raising and fishing since changes in ocean temperature affect fish breeding.

1.3.3.4 Ecosystems

Changes in climate also affect people and living organisms through changes in ecosystems. Ecosystems encompass the interaction of living organisms and the non-living components of their surroundings. These include air, soil, water and sunlight. Sustainable economic growth and human wellbeing depend on ecosystems. For instance, changes in water flow and availability, which is one component of ecosystem, will affect the balance of entire ecosystem of a place. Human actions and climate change aggravate the pressure on ecosystems. For example, reefs, mangroves, and barrier islands provide a defence mechanism on coastal ecosystems against storm surges (Groffman et al., 2014).

Climate is an important environmental influence on ecosystems. Climate changes and the impacts of climate change affect ecosystems in a variety of ways. For instance, warming could force species to migrate to higher latitudes or higher elevations where temperatures are more conducive to their survival. Similarly, as sea level rises, saltwater intrusion into a freshwater system may force some key species to relocate or die, thus removing predators or prey that were critical in the existing food chain.

1.3.3.5 Coastal Zones

Coastal ecosystems aid in providing a source of food for both coastal dwellers and other organisms found in the coastal zones. They are also essential in regulating coastal chemical cycles (Senga, Kihupi, Liwa & Kimaro, 2014).

Most storms, heavy rainfall and warmer temperatures tend to affect the coastal zones. Sea level changes obviously take place in coastal areas and affect ecosystems and individuals living in the coastal areas. Additionally, the excess carbon dioxide concentrations in the air are absorbed by the oceans and change the pH of the ocean to acidic (EPA, 2014).

Coastal flooding and erosion are among other negative impacts of climate change in coastal zones. The increase of ocean temperatures results in coral bleaching and mortality. Thermal expansion of ocean water causes sea level rise which then contaminates the fresh water with sea water and croplands in the coastal areas (Nicholls et al., 2007).

1.3.3.6 Settlements, Industry, Infrastructure and Society

Extreme weather events such as storms, heavy snow and floods affects most infrastructures such as transport systems and settlements during onset. Agricultural and forest product industries also tend to be affected by climate change induced events. Floods and snows shortens the life expectancy of roadways and highways and other infrastructures such as railway lines and even roadways (EPA, 2014). Natural resource industries such as food and paper industries will also be hit by climate change.

Urban dwellers are more affected by climate change events. Due to high population densities in urban areas and higher heat absorption in urban areas, heat waves tend to be stronger in urban areas than rural areas.

Climate change will also affect other industries such as energy sector. Energy production, energy consumption and even cost associated with the two will change with the change of climate (Wilbanks et al., 2007). Tourism and recreational industries are also affected, as coastal flooding, storm surges and sea level rises will affect tourism sector in beaches. Skiing and snowmobiling might take a hit due to the decrease of a number of snowy days. Forest fires will likely affect camping and hiking activities. Changes in animals and fish migration pattern due to climate change will also affect fishing and hunting activities (EPA, 2014).

CHAPTER TWO
STUDY AREA AND DATA DESCRIPTION

2.1 Study Area

The study area is Unguja which is the main Island of the two that form Zanzibar. The Island has a total area of 1666 sq. km and is located 40 km off the East African coast, between 5°and 6° south latitudes and along 39° and 40° east longitudes. The north- south extent of Unguja is approximately 85 kilometres with the width in east-west direction varying from 9 km in the northern end to about 35 km in the south (Hettige, 1990).

2.1.1 Population

The population of Zanzibar Island is 896,721 according to 2012 census, with an annual growth rate of 3.13. An approximate 46% of the population is living in urban areas. The total number of households is 175,186 with an average household size of 5.1. The population density in Zanzibar Urban West is 2,600/km^2.

The entire population of Zanzibar is growing at a rate of 2.8% annually which is very high even by African standards. At this rate, the population of Zanzibar is estimated to double by the year 2036.

2.1.2 Climate

The climate of Unguja Island is equatorial maritime climatic regime and sunshine of over 2000 hours per year. Unguja Island experiences a bimodal rainfall pattern with the annual average of 1600mm. The two main rainy seasons are locally known as Masika (long rains) between March and May and Vuli short rains (October-December).

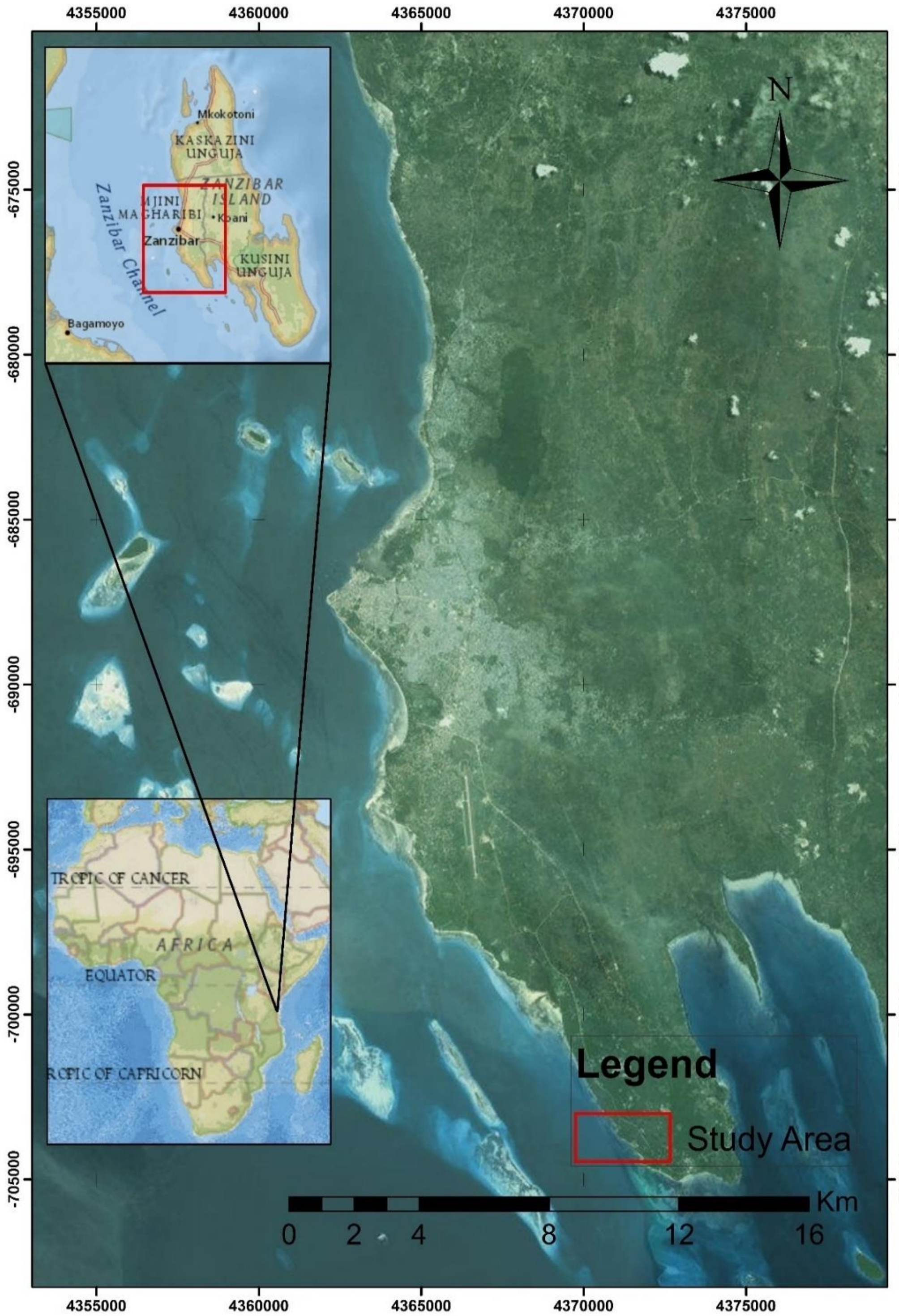

Figure 2.1 Map of Unguja Island showing the study area

Annual average temperature of the island is 26 °C. The maximum average temperature of 27 °C occurs in January and minimum average temperature of 24 °C occurs in July. The average daily evaporation for Unguja is 5mm. This rises from 4.4 mm in April to 5.8 in February (Tanzania Metrological Agency [TMA], 2015).

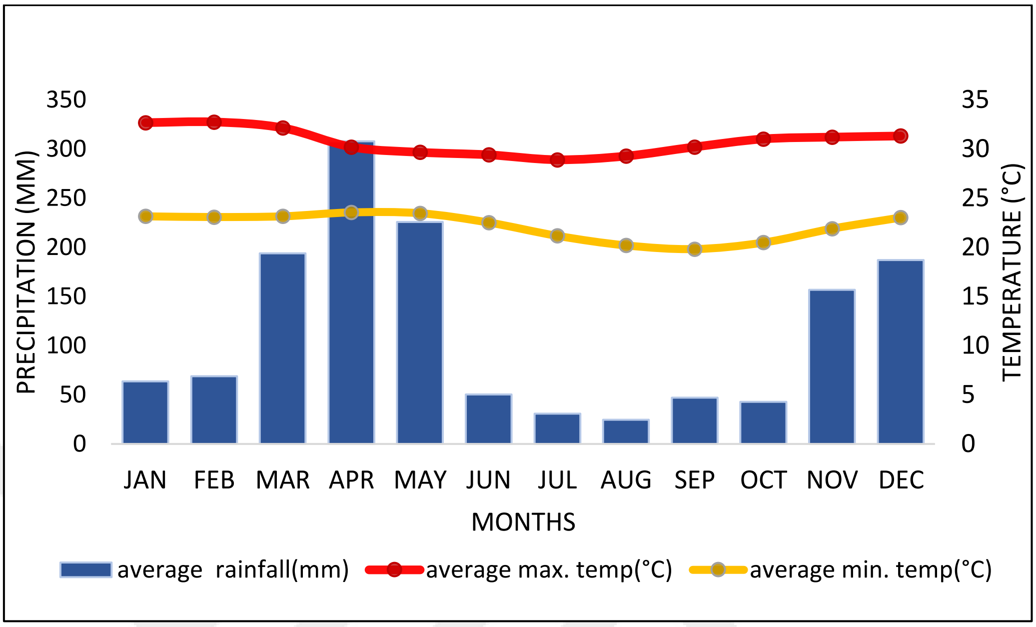

Figure 2.2 Average Annual Climate on Unguja island (TMA, 2015)

2.1.3 Topography

Unguja Island is fairly flat characterized by series of corridors and residual hills running in North-South direction, the highest point being 119 metres above sea level. The western part is fertile and the other part is coral in nature (Hettige, 1990).

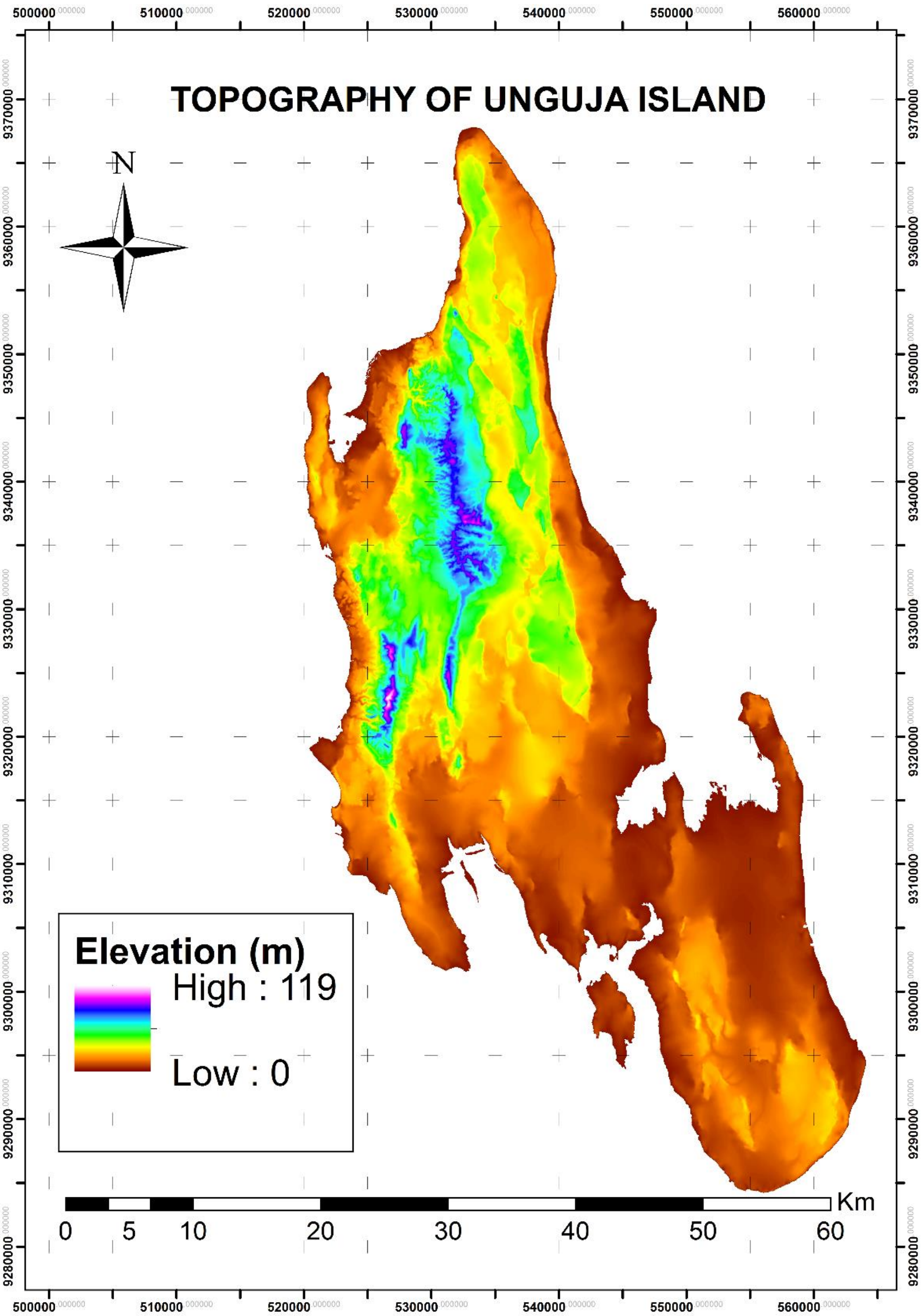

Figure 2.3 Map showing a topographyof Unguja island

2.1.4 Vegetation and Drainage

The western side of the ridge is fertile with large plantations of coconuts, cloves and agroforests. Whereas the eastern part is dominated by mangrove swamps, scrubs, coral rag and grasslands. There is only one stream in the whole coral area. A good number of streams are found on the fertile western side. These include Kipange, Mwanakombo, Zingwezingwe and Mwera streams (Hettige, 1990).

2.2 Climate Change in Unguja

This section will give a brief explanation of the current state of climate change in Zanzibar, examine the recorded and future climate trends and summarizes the impacts of climate change in Zanzibar. In addition, the efforts taken by the government of Zanzibar to curb the negative impacts of climate change will be presented.

2.2.1 Current State of Climate Change in Unguja Island

The coastal areas and small islands like Zanzibar islets are among the areas that are most affected by climate change. This is exacerbated by the lack of improper adaptation programs due to lack of funds and awareness of the climate change problem. Most of the funds, in countries like Zanzibar, are allocated to other poverty-alleviating programs instead of curbing climate change and its related effects. However, the climate change impacts pose challenges to the economic growth of Zanzibar as a country and socio-economic well-being of its citizens.

Studies have indicated that Zanzibar, as most of the world, has recorded climate readings that prove the change in our climate. These changes include increase in temperature, rainfall and sea-level readings in both recorded measurements and models predicting future climate changes.

The Zanzibar government has identified areas such as water availability, food security and human health and tourism to be under very imminent threat due to the negative effects of climate change and global warming.

2.2.1.1 *Climate Change Indicators in Unguja Island*

This section will provide a quick insight into the climate condition of Unguja Island by studying and identifying climate change indicators in Unguja Island.

2.2.1.1.1 Temperature. Zanzibar has witnessed an observed climb in temperatures from the observed records over the past 40 years, as an increase in average monthly and yearly temperatures, especially average minimum as can be seen in Figure 2.5. The highest recorded temperature on the island was recorded on 27th February of 2007 at 39.4 °C (TMA, 2015). An overall increase of 1.9 °C between 1961 and 2005 has been reported by TMA.

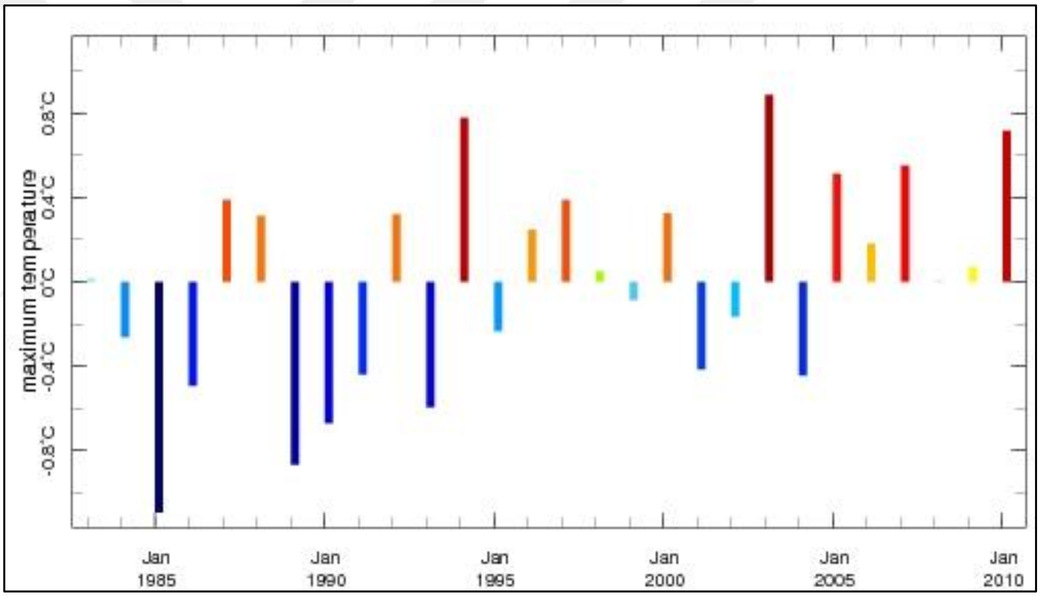

Figure 2.4 Average maximum temperature on Unguja island, 1983 - 2010 (TMA, 2015)

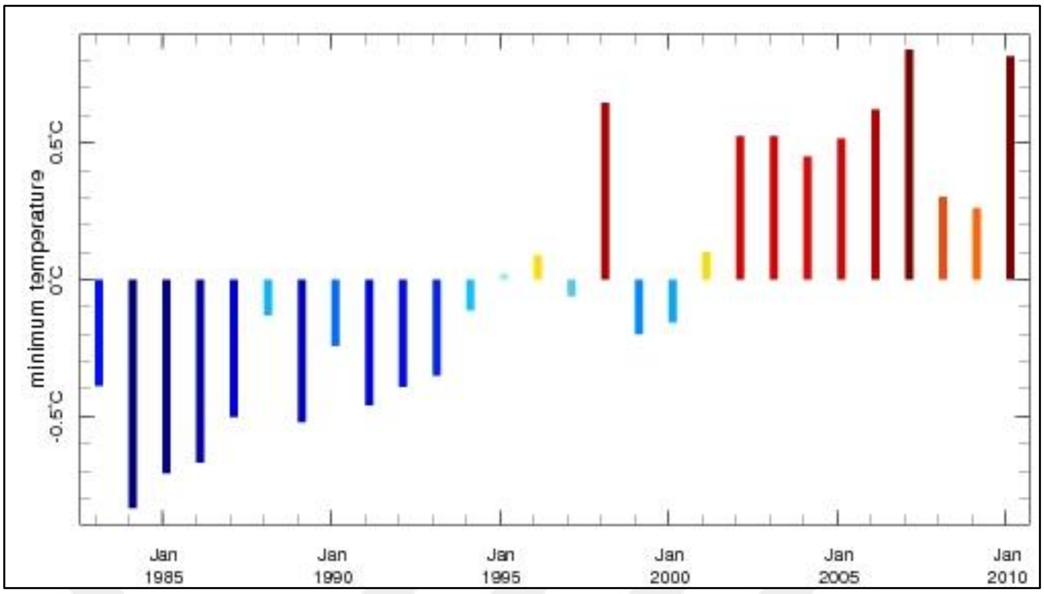

Figure 2.5 Average minimum temperature on Unguja island, 1983 - 2010 (TMA, 2015)

2.2.1.1.2 *Rainfall*. Rainfall has had an erratic pattern with unpredictable trends on Unguja Island. There has been a slight decrease in measured rainfall amount coupled with very high rainfall records in the past decade. Likewise, there has been an increase of thunderstorms and heavy rain showers between months of March and May in the recent years. For example, Victoria garden metrological station recorded 471 mm of rainfall in 24hrs on 16th April 2005, which was the highest measurements in 50 years in Unguja Island (TMA, 2015). Observations also indicate that the total number of rainy days has significantly decreased, whereas the intensity of rainfall has increased.

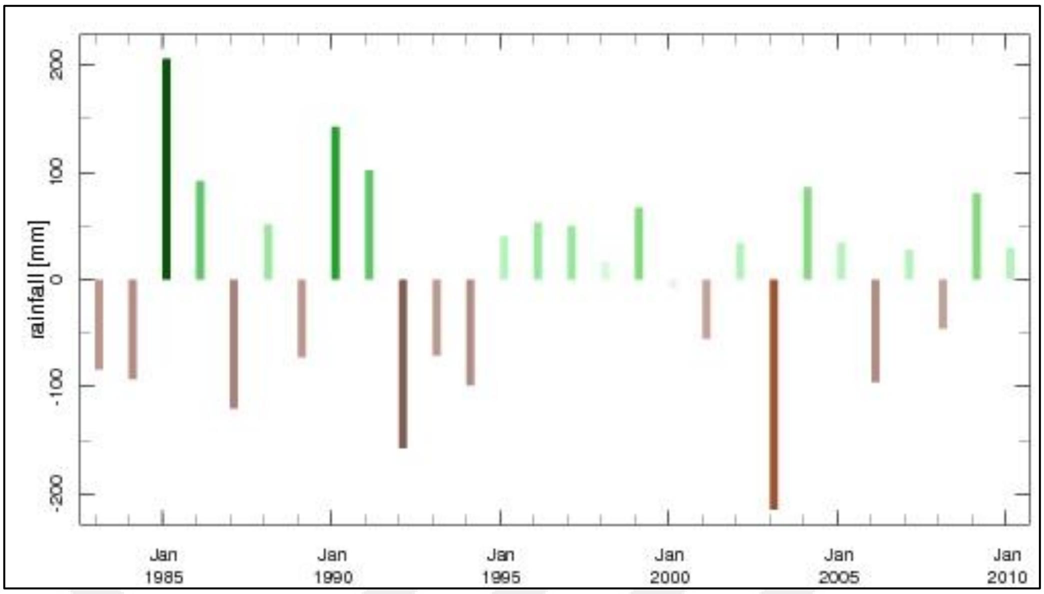

Figure 2.6 Annual rainfall on Unguja island, 1983 - 2010 (TMA, 2015)

2.2.1.1.3 Sea Level Rise. Sea level rise is also used as an indicator for climate change. Thermal expansion of water due to increased temperatures and melted glacial ice increase the volume of sea water. Globally satellite measurements recorded and an increase of sea level of 3.2 mm per year between 1993 and 2012. For the case of Unguja Island, the same pattern of sea level rise has been observed using tide gauge data collected daily. However, inter-annual and decadal fluctuations are responsible for the decrease in sea level as seen in Figure 2.7 between the 1990s and early 2000s.

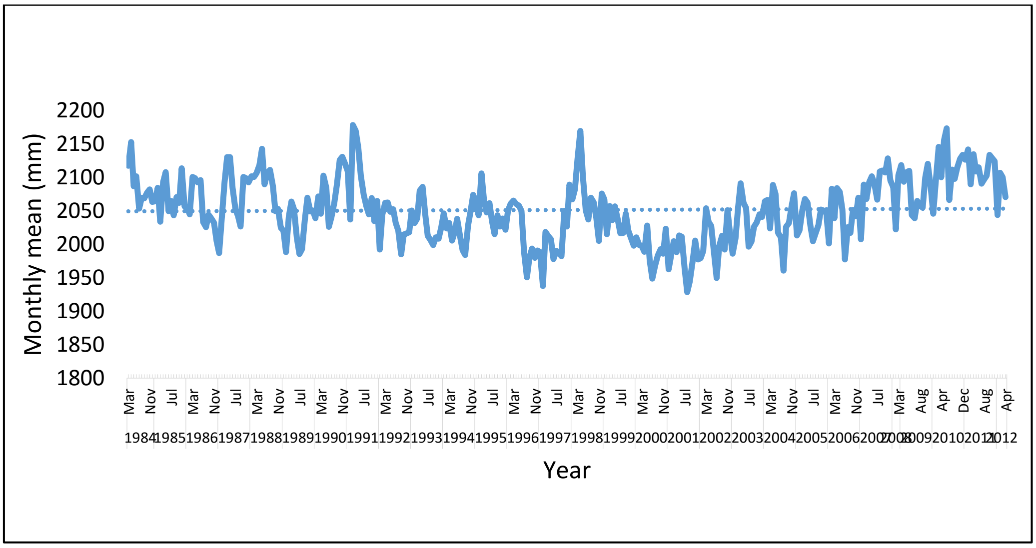

Figure 2.7 Monthly Mean sea level (mm) on Unguja island, 1984 - 2012

2.2.1.2 Climate Change Impact in Unguja Island

This section will give an explanation of some of the impacts of climate change observed on Unguja Island.

Chapter 1 gave an explanation of the effects of climate change as it affects global dynamics, therefore the impacts are more generalized as their effects differ depending on the region being investigated. However, in this section detailed impacts of the effects and negative consequences of climate change will be explained as reported in Zanzibar or more specifically on Unguja island. These impacts have affected a wide range of sectors raging from socially, culturally to economically and environmentally.

In all circumstances, the identification and categorization of these impacts is very essential in tackling and curbing the effects of climate change in Zanzibar.

2.2.1.2.1 Coastal Zones. Coastal zones are affected by salt water intrusion due to increased wave heights and strong winds. This in turn affects fresh water quality due to salt water intrusion. In addition, farm lands near the sea are also affected by the sea water intrusion rendering them unsuitable for agriculture. More than 17 sites were identified to be affected by salt water intrusion on Unguja Island.

2.2.1.2.2 Fishery and Marine Ecosystem. Unguja has a diverse marine ecosystem consisting of coral reefs, sea grasses and mangrove vegetation. These marine ecosystems provide economic support to the coastal residents on Unguja Island. Economic activities in these areas include fishing, seaweed farming, mangrove harvesting, snorkelling and tourism in general. Destruction of coral reefs from bleaching together with warming affect fish breeding and resting places, have created a decline in the fishery. Fishery contributes to the economy both in terms of income and providing employment opportunity.

2.2.1.2.3 Agriculture. Salt water intrusion into farmlands, changes in rainfall patterns and amount, and other climate changes have affected crop growth and harvests. Unguja Island depends to a great extent on agriculture with cloves and coconut export contributing significantly to the total exports. Most people grow food crops for their own consumption and to supplement their incomes. Since Unguja Island economy depends on agriculture, negative impacts of climate change might have negative effects on its economy (Mbilinyi, Saibul & Kazi, 2013).

Changes in rainfall pattern especially between 2006 and 2007 affected agriculture output on Unguja Island and led to a decrease in crop production. These changes in rainfall also led to a drought resulting in animal deaths in some areas due to lack of grazing lands, which in turn reduced milk production and beef availability.

2.2.1.2.4 Health. Diseases such as cholera and malaria are directly related to changes in climate. Floods and drought tend to affect water availability hence, causes risk of water-borne diseases such as malaria (due to increase of mosquitoes breeding places) and diarrhoeal diseases. The increase of water-related diseases was witnessed in 2007 erratic rainfall pattern and flooding that contaminated water sources.

2.2.1.2.5 Water Resources. Coastal flooding and changes in rainfall patterns affect the quality and availability of water, since Unguja depends on rainfall and underground water supplies for its drinking water. Cave waters are also affected by high concentration of nutrients due to sea water intrusion. Some caves have reported higher values of contamination than those recommended for drinking by WHO (Ali, Nyakairu, & Vuai, 2012) due to sea water intrusion from tidal change and sea level rise.

2.2.1.2.6 Forests. Generally, a decrease in rainfall amount has led to decrease in forest coverage in Unguja Island. The decrease in ground water levels in Jozani forest, the largest forest in Unguja Island caused the creation of sub-climate conditions that changed species composition. Also, loss of forest areas causes erosion which in turn deposit sediments in coastal water that cause the loss of marine life (Wang, et al., 2005).

2.2.1.2.7 Infrastructure. Flooding from heavy rains and increasing strong winds contributes to the destruction of infrastructures such as schools, roadways, waste disposal, and water supply systems.

2.2.1.3 Adaptation and Mitigation

The government of Zanzibar in order to tackle and curb the impacts of climate change, has established a Disaster Management Commission. Together with this climate change strategy was also put in place, it is expected to achieve sustainable development by 2020. One of Zanzibar Strategy for Growth and Poverty Reduction of Poverty (ZSGRP) operational targets is to set a capacity target for climate change impact and adaptation by 2015 (The Revolutionary Government of Zanzibar, 2007) .

The policies and current actions being implemented focus on monitoring coastal erosion and analysing the damage caused by erosion. The action plan for coastal zones protection includes the building of dykes and physical barriers to stop and discharge the flooded zones in coastal areas. Other plans include vegetation restoration in coastal areas (mangroves plantation, and sea grasses replanting).

Monitoring and research being conducted in order to understand and arrive at new ways to protect against climate change impacts. This includes providing education to citizens through awareness programs concerning the severity of the problem and how they can help to protect the coastal ecosystems.

Plans to research and adopt the use of improved seeds for drought resistance crops are underway in order to deal with the lack of rainfall.

In order to protect water resources, alternative water supply programmes and water harvesting schemes have been proposed. A pilot project is underway on Unguja Island to supply villagers in Nungwi village by constructing a new water supply pipeline to provide fresh water for the village since their traditional fresh water sources have been affected by salt water intrusion due to sea level rise.

Other adaptation and mitigation plans include sustainable tourism and plans to reduce carbon dioxide emissions on Unguja Island.

2.2.2 Future Trend

Climate change predictions models such as Regional Climate Models (RCMS) are showing that there will be a further increase in monthly temperature of up to 2 °C by the 2050s and even a higher increase by the 2090s. This increase exceeds the previous rates of change observed over the previous 40 years.

The same predictions are also being observed with the current rainfall patterns, with future trends that show a complex and complicated trend. Models predict a decrease in precipitation and number of rainy days by the 2050s. However, it is predicted that annual rainfall will increase in the early months of the year with an abrupt decrease in the following months.

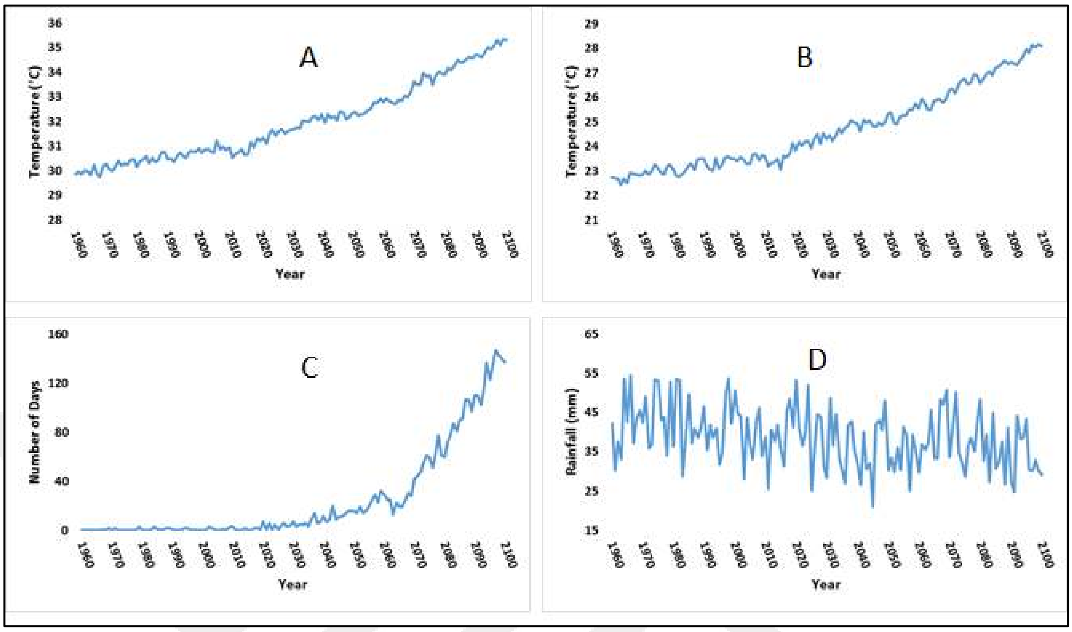

Figure 2.8 Future climate change prediction using RCP8.5 model, A) Average maximum temperature, B) Average minimum temperature, C) Number of days with temperatures above 36 °C, D) Maximum daily rainfall

Sea level rise is also projected to increase globally by up to 1 meter and between 18 – 59 cm in Unguja Island, with erratic changes in wind patterns and wave regimes that could further exacerbate its effects. Sea surface temperatures and ocean acidification are also expected to increase.

2.3 Data Description

The study combined the use of both remotely sensed data and metrological data collected by Tanzania Metrological Agency (TMA), Zanzibar office. Remotely sensed data used is from Landsat satellite collection archive, while the metrological data was obtained in excel format and MS excel software was used to analyse the data.

Moreover, other data such as sea level data, coastline shapefiles for land-sea demarcation, elevation datasets were also used in the analysis section of this thesis.

2.3.1 Remote Sensing Data

Landsat imagery collected from Landsat 5 mission for our study area were downloaded from the U.S Geological Survey website. The purpose of this data was mainly for visual analysis and classification purposes and creating indices for other related analysis. These indices and classified Landsat imagery were then compared with the official metrological data collected by TMA for further analysis.

2.3.1.1 Landsat Mission

The legacy Landsat satellites date back to 1972 as an earth observing mission which was started with Landsat 1, since then the mission has continued to capture space-based images of the Earth's continental and coastal landscapes providing data valuable for assessing impacts of human actions and natural changes. The wide applicability of this data includes it application in agriculture, forestry, regional planning and climate change. These changes can be monitored and characterized in temporal dimension.

This mission is a joint initiative of the National Aeronautics and Space Administration (NASA) and the U.S Geological Survey (USGS). NASA's task is to construct the satellites and its sensors and then launch them to the space and validate their performance. The USGS assumes ownership and operation of the satellites and manages collection distribution and archiving of the data.

The open and free huge archives of Landsat data are essential in management of land resources such as in flood and wild fires mitigations, forest and agricultural management, storm and flood extent. They can also be used in mapping urban expansions and study of climate changes such as measuring extent of polar ice and their melting rate.

The Landsat project was conceived in the mid-1960s by Department of the Interior, NASA and The Department of Agriculture aiming at launching the first civilian earth observing satellite that was materialized on 23 July, 1972 with the launch of the Earth Technology Satellite (ERTS-1), which was then renamed Landsat 1.

The launch was then followed by the launches of Landsat 2 to Landsat 8. However, Landsat 6 failed to reach orbit in 1993. Landsat 5 set a new Gunnies World for "longest-operating Earth observation satellite". Landsat 7 and Landsat 8 continue the mission of providing global data. Landsat 9 is planned to be launched in 2023 (U.S. Geology Survey, 2015).

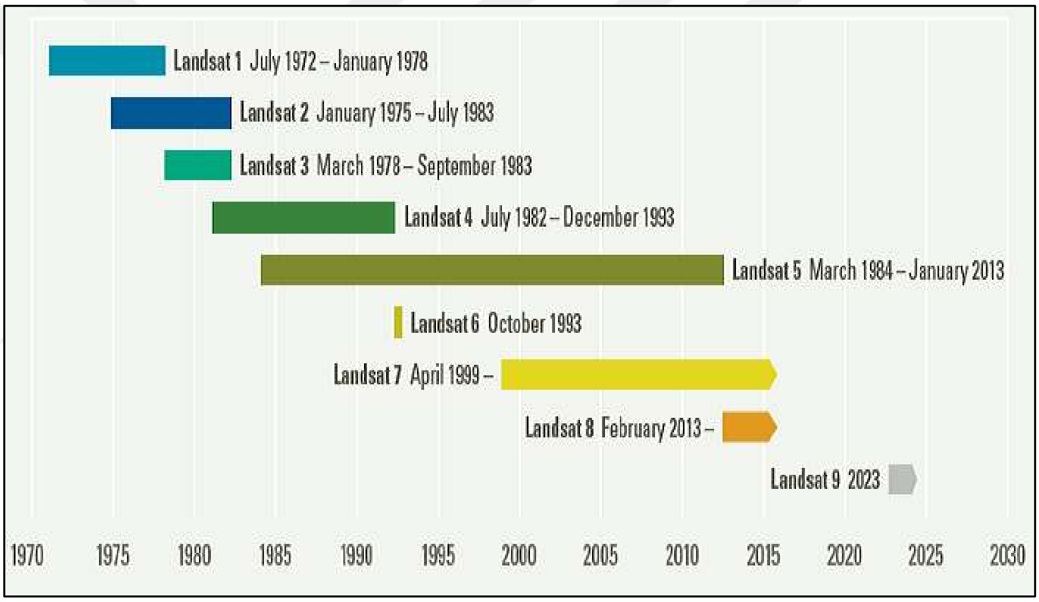

Figure 2.9 Timeline and history of the Landsat Missions

2.3.1.1.1 Satellite Acquisitions. Landsat 1, 2 and 3 orbit nominally at an altitude of 900 km with a period of revolution of 103 minutes (approx. 14 orbits per day). The three satellites cross the equator nominally at 9:42 local time in descending mode, yielding repeat coverage every 18 days.

Landsat 4, 5, 7 and 8 orbit the earth at an altitude of 705 km with a period of revolution every 99 minutes. Equatorial crossing time is nominally 9:45 AM (± 15 minutes) local time in descending node. All of these four satellites yield a repeat coverage of 16 days (U.S. Geology Survey, 2015).

2.3.1.1.2 Sensors and Band Designations. The sensor on-board Landsat 1, Landsat 2, and Landsat 3 was the Multispectral Scanner (MSS), collecting imagery at a resolution of 79 meters in four spectral bands ranging from the visible green to the near-infrared (IR) wavelengths. The processed data are resampled to 60 meters. Delivered Landsat MSS data are resampled to 60 meters.

Landsat 4 and Landsat 5 had two types of sensors on-board, the Multispectral scanner and Thematic Mapper (TM). The TM sensor was comprised of added bands in the shortwave infrared (SWIR) part of the spectrum. Both satellites had visible bands having a spatial resolution of 30 meters, near-infrared and short-wave infrared bands. In additional to these bands, there is a 120-meter of thermal infrared band. There is spatial resolution of 30 meters for the visible, near-IR, and SWIR bands; and the addition of a 120-meter thermal IR band. Delivered Landsat 4 and Landsat 5 TM thermal data are resampled to 30 meters.

Landsat 7 carries the Enhanced Thematic Mapper Plus (ETM+), with 30-meter visible, near-IR, and SWIR bands; a 60-meter thermal band (resampled to 30m); and a 15-meter panchromatic band.

Landsat 8 carries the Operational Land Imager (OLI) and the Thermal Infrared Sensor (TIRS). OLI collects data with a spatial resolution of 30 meters in the visible, near-IR, and SWIR wavelengths, and a 15-meter panchromatic band as in Landsat 7. OLI also contains a deep blue band for coastal-aerosol studies and a band for cirrus cloud detection. The TIRS contains two thermal bands, designed to allow the use of split-window surface temperature retrieval algorithms and a Quality Assessment (QA) band is also included in Landsat 8 data products (U.S. Geology Survey, 2015).

Table 2.1 Display and comparison of the bands and wavelengths of each Landsat sensor

Band Designations	LANDSAT BAND WAVELENGTH COMPARISONS All bands 30-meter resolution unless noted									
	L8 OLI/TIRS		L7 ETM+		L4-5 TM		L4-5 MSS*		L1-3 MSS*	
Coastal/Aerosol	Band 1	0.43 - 0.45	--	--	--	--	--	--	--	--
Blue	Band 2	0.45 - 0.51	Band 1	0.45 - 0.52	Band 1	0.45 - 0.52	--	--	--	--
Green	Band 3	0.53 - 0.59	Band 2	0.52 - 0.60	Band 2	0.52 - 0.60	Band 1	0.5 - 0.6*	Band 4	0.5 - 0.6*
Panchromatic	Band 8**	0.50 - 0.68	Band 8**	0.52 - 0.90	--	--	--	--	--	--
Red	Band 4	0.64 - 0.67	Band 3	0.63 - 0.69	Band 3	0.63 - 0.69	Band 2	0.6 - 0.7*	Band 5	0.6 - 0.7*
Near-Infrared	Band 5	0.85 - 0.88	Band 4	0.77 - 0.90	Band 4	0.76 - 0.90	Band 3	0.7 - 0.8*	Band 6	0.7 - 0.8*
Near-Infrared	--	--	--	--	--	--	Band 4	0.8 - 1.1*	Band 7	0.8 - 1.1*
Cirrus	Band 9	1.36 - 1.38	--	--	--	--	*Acquired at 79 meters, resampled to 60 meters			
Shortwave Infrared-1	Band 6	1.57 - 1.65	Band 5	1.55 - 1.75	Band 5	1.55 - 1.75	** 15-meter (panchromatic)			
Shortwave Infrared-2	Band 7	2.11 - 2.29	Band 7	2.09 - 2.35	Band 7	2.08 - 2.35	T1 = Thermal (acquired at 100 meters, resampled to 30 meters			
Thermal	Band 10 T1	10.60 - 11.19	Band 6 T2	10.40 - 12.50	Band 6 T2	10.40 - 12.50	T2 = Thermal (acquired at 120 meters, resampled to 30 meters			
Thermal	Band 11 T1	11.50 - 12.51	--	--	--	--	-- = not applicable			

Table 2.2 The bands of each Landsat satellite and descriptions of how each band is best used.

[--, not applicable]						
Uses of Landsat Bands						
Band Name	L8 OLI/TI	L7 ETM+	L4-5 TM	L4-5 MSS	L1-3 MSS	Description of use
Coastal/Aerosol	Band 1	--	--	--	--	Coastal areas and shallow water observations; aerosol, dust, smole detection studies.
Blue	Band 2	Band 1	Band 1	--	--	Bathymetric mapping; soil.vegetation discrimination, forest type mapping, and identifying manmade features.
Green	Band 3	Band 2	Band 2	Band 1	Band 4	Peak vegetation; plant vigor assesments.
Red	Band 4	Band 3	Band 3	Band 2	Band 5	Vegetation type identificartion; soils and urban features.
Near-Infrared	Band 5	Band 4	Band 4	Band 3	Band 6	Vegetation detection and analysis; shoreline mapping and biomass content.
	--	--	--	Band 4	Band 7	
Shortwave Infrared 1	Band 6	Band 5	Band 5	--	--	Vegetation moisture content/drought analysis; burned and fire-affected areas; detection of active fires.
Shortwave Infrared 2	Band 7	Band 7	Band 7	--	--	Additional detection of active fire (especially at night); plant moisture/drought analysis.
Panchromatic	Band 8	Band 8	--	--	--	Sharpening multispectral imagery to higher resolution.
Cirrus	Band 9	--	--	--	--	Cirrus cloud detection.
Thermal	Band 10	Band 6	Band 6	--	--	Ground temperature mapping and soil moisture estimations.
	Band 11			--	--	

2.3.1.1.3 Landsat Data Products and Processing. The data from USGS archives is geometrically, radiometrically and ortho-corrected. Millions of Landsat scenes have been downloaded freely by users worldwide.

The parameters used in processing data products known as level 1 data include the use of convolution resampling, projecting the data into Universal Transverse Mercator

(UTM) projection system, and World Geodetic System (WGS) 1984 datum and the use of north-up map orientation. The products are delivered in Georeferenced Tagged Image File Format (GeoTIFF) in archived file format. The size of the data varies from sensors as the newer sensors tend to produce huge data volumes due to additional bands. Higher level data products also known as Level 2 are available on request. These data products are used for temporal observation in studying the impact of climate change. Examples of such data include surface reflectance-based spectral indices (U.S. Geology Survey, 2015).

2.3.1.1.4 Obtaining Landsat Data Products. Landsat Level 1 data is freely available from USGS archives through EarthExplorer website (http://earthexplorer.usgs.gov) and GloVis (http://glovis.usgs.gov). The former also provides bulk downloading capabilities.

2.3.1.2 Characteristics of Data Used for This Study

The Landsat imagery used in this analysis were downloaded from EarthExplorer website (http://earthexplorer.usgs.gov). Obtaining cloud-free imagery was a very difficult since the study area is located in tropical region characterized by sky with heavy clouds and excessive humidity. Despite this setback, three imageries with the lowest percentage of clouds were downloaded. The Landsat 5 scene obtained on 01 July 2009 is the only scene that covers the island of Unguja without clouds since the inception of Landsat mission. Table 2.3 summaries the characteristics of the downloaded Landsat data.

Table 2.3 Landsat data used in this study

Acquisition Date	**Sensor**	**Sun Elevation (Degrees)**	**Sun Azimuth (Degrees)**	**Cloud Cover (%)**
01 July 2009	TM	47.74	45.76	17

2.3.1.3 Pre-processing of Landsat Imagery

The pre-processing is essential in removal of unwanted artefacts that could be present in our data, it is also important for some of our analysis, for example the development of indices yield better results when the raw Digital Numbers have been converted to surface reflectance. In the pre-processing, the DN values recorded in the digital image were converted to spectral radiance (at the sensor), then the spectral radiance was converted to apparent reflectance (also at the sensor), which is finally converted to reflectance at the Earth’s surface (top-of-atmosphere reflectance) by removing atmospheric effects due to scattering and absorption (Song, Woodcock, Seto, Lenney & Macomber, 2001).

2.3.2 Climate Data

Data provided by TMA included rainfall data, temperature data and wind data in excel format. The data included monthly minimum and maximum readings for temperature data and total recorded rainfall for each month between the years 2000 to 2010. Although the interval is somewhat short, it was expected to paint a quick and rough picture of the climate pattern for our study area (U.S. Geology Survey, 2015).

2.3.3 Other Data

In addition to remote sensing and metrological data, sea level data for Unguja Island was downloaded in text format from University of Hawaii Sea Level Centre (UHSLC) and other GIS data for the entire island of Unguja was obtained from Department of Survey and Urban Planning (DoSUP), Zanzibar. These included the followings: topographic maps 1984 (1:10,000), coastline shapefiles (vector) that was used for study area delineation, forest inventory maps (GeoTIFF) from Department of Forest and Natural Resources (DFNR) and orthoimagery of 2004 from DoSUP both used to help in classification and accuracy assessment. All these GIS data were obtained either in vector format or raster format. The projection system in both data formats is Universal Transverse Mercator (UTM) projected on Arc1960 datum. This projection system is locally used for the study area in our analysis.

CHAPTER THREE
METHODOLOGY

The software used in this analysis was ERDAS IMAGINE 2011, ArcMap 10 and Microsoft Excel 2010. The pre-processing of the data was done using ERDAS IMAGINE 2011, and the actual analysis was performed in ArcMap 10 and Microsoft Excel 2010 was used for analysis of metrological and sea level data.

3.1 Radiometric and Atmospheric Correction

The processing of all the acquired Landsat scenes was done using ERDAS IMAGINE software. The mentioned software has models and extensions dedicated to performing pre-processing of remotely sensed data. ATCOR extension is a spatially-adaptive fast atmospheric correction algorithm for a flat terrain working with an atmospheric database model for atmospheric correction of medium and high resolution satellite sensors, which removes atmospheric artefacts in the scene. The software is used to derive surface reflectance, emissivity and brightness temperatures from calibrated images. ATCOR uses SPECTRA which is used for determination of an appropriate atmosphere i.e. aerosol and humidity and the decision on the selected visibility. The other functionality is atmospheric correction in which the user specifies the atmospheric condition of an area of the image and a comparison between scene-derived spectra and reference spectra from the spectral library can be made to acquire the best and most suitable conditions. ATCOR incorporates the Moderate Resolution Transmission (MODTRAN) 4 radiative transfer code. The MODTRAN4 code is an example of advanced atmospheric radiative transfer code, that provides accurate calculations by using a rigorous mathematical formula and a fine spectral resolution (Guanter, Ritcher & Kaufamann, 2009). ATCOR was also used to convert thermal band images DN to brightness temperatures, the output was used in Landsat Surface Temperature Estimation. Prior to using ATCOR a radiometric calibration was performed. This is a straight forward process in ERDAS IMAGINE software by using the radiometric calibration tool that gives options of converting the DN values to spectral radiance or a direct conversion to apparent reflectance.

Prior to using ATCOR, the original scenes were projected into Universal Transverse Mercator (UTM) projected on WGS1984 37S, then the images were clipped using the study area shapefile so as to improve the accuracy of the results. The software uses metadata in the header files from the acquired scenes to determine the correct attributes (Gains, offsets, solar irradiance, solar elevation, solar zenith, zenith azimuthal and acquisition time) needed for the correction (Du, Teillet & Cihlar, 2002).

The process was repeated for all acquired imagery. The obtained reflectance bands were then imported to ArcMap 10 where the study area shown in Figure 2.1 was clipped from the whole scene.

3.2 Development of Indices

Two indices were used in this analysis. These are Normalized Difference Vegetation Index (NDVI) and Normalized Difference Built-Up Index (NDBI). The development of this analysis will provide a way to establish a relationship between metrological data collected by TMA in Zanzibar. Not only that, the indices will also be used as intermediate input in creating Land Surface Temperature raster file that will also be used to establish relationship between the created raster and the indices themselves.

3.2.1 Normalized Difference Vegetation Index (NDVI)

The NDVI index was first applied by Rouse et al, (1973). It was used as a measure of vegetation distribution in an area. Vegetation coverage has an effect on the local and regional climate pattern of an area. NDVI has been widely used in conjunction with other techniques to study the changes in Land surface temperatures. Originally, it was developed using Landsat TM bands 4 (NIR Band) and 3 (Red Band). NDVI ranges from values of positive (+1) to negative 1 (–1), whereas, higher NDVI values are associated with dense vegetation, soil and urban have values close to zero while water is normally associated with negative values.

$$NDVI = \frac{(NIR - RED)}{(NIR + RED)} \quad (3.1)$$

The use of NDVI in vegetative studies such as in crop yields, pasture performances, vegetation type and condition and estimation of biomass amount would provide a way to determine changes in vegetated areas between two images and their effect to the change of climate.

3.2.2 Normalized Difference Built-Up Index (NDBI)

This index is used to monitor the growth and distribution of urban and/or built up areas. The development of the index was based on the uniqueness of spectral response of built-up lands of having higher reflectance in SWIR wavelength range than in NIR wavelength range (Xu, 2007). The use of NDBI also includes the measuring of urban development intensity and more importantly, an indicator for urban impervious surface in which sensible heat exchange takes place the most (Li & Liu, 2008).

$$NDBI = \frac{(SWIR - NIR)}{(SWIR + NIR)} \quad (3.2)$$

Originally, NDBI was developed to be used with Landsat TM bands 5 and 4. However, it can be used with any multispectral sensor with a SWIR band between 1.55-1.75 µm and a NIR band between 0.76-0.9 µm.

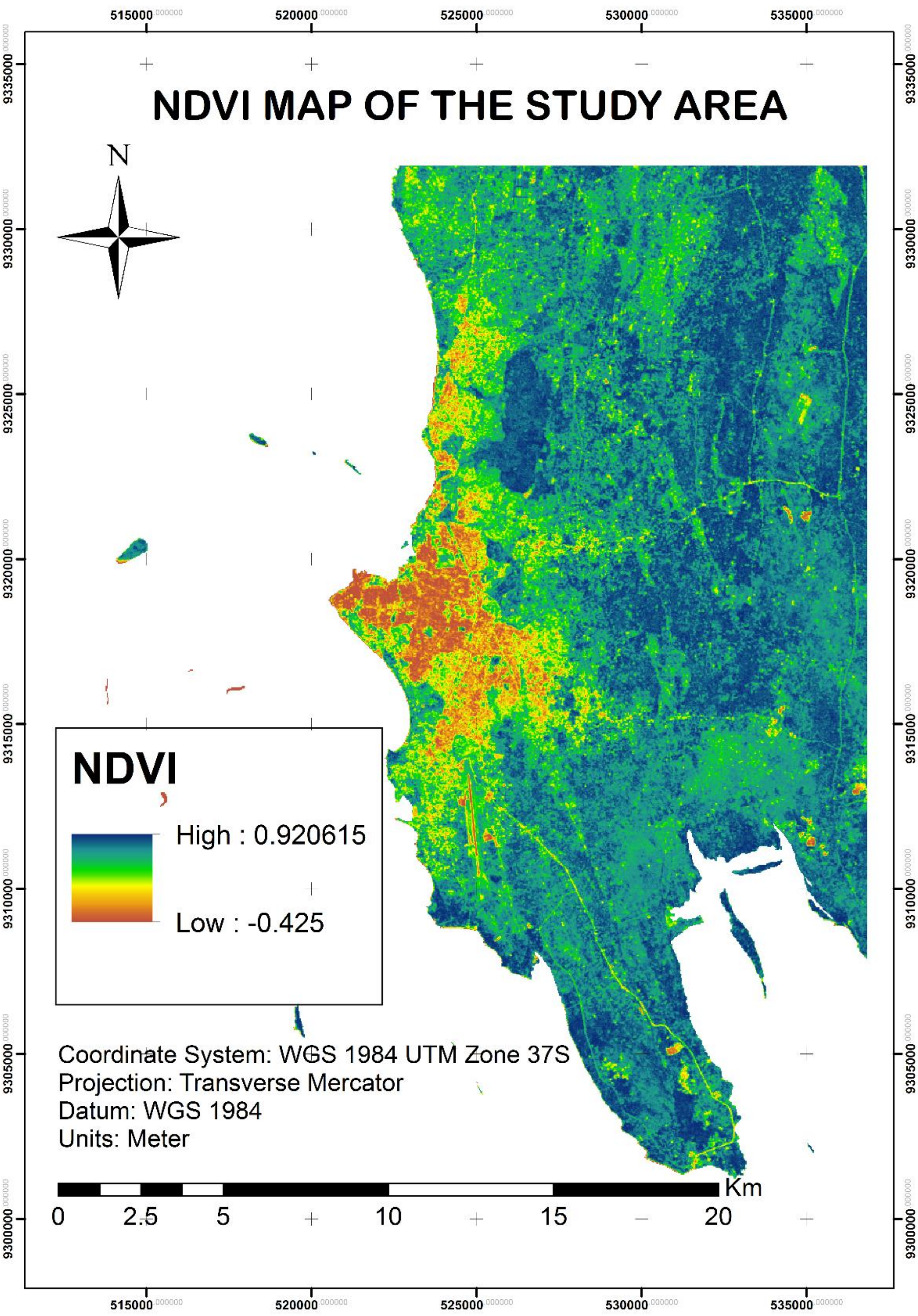

Figure 3.1 NDVI image of study area using Landsat TM

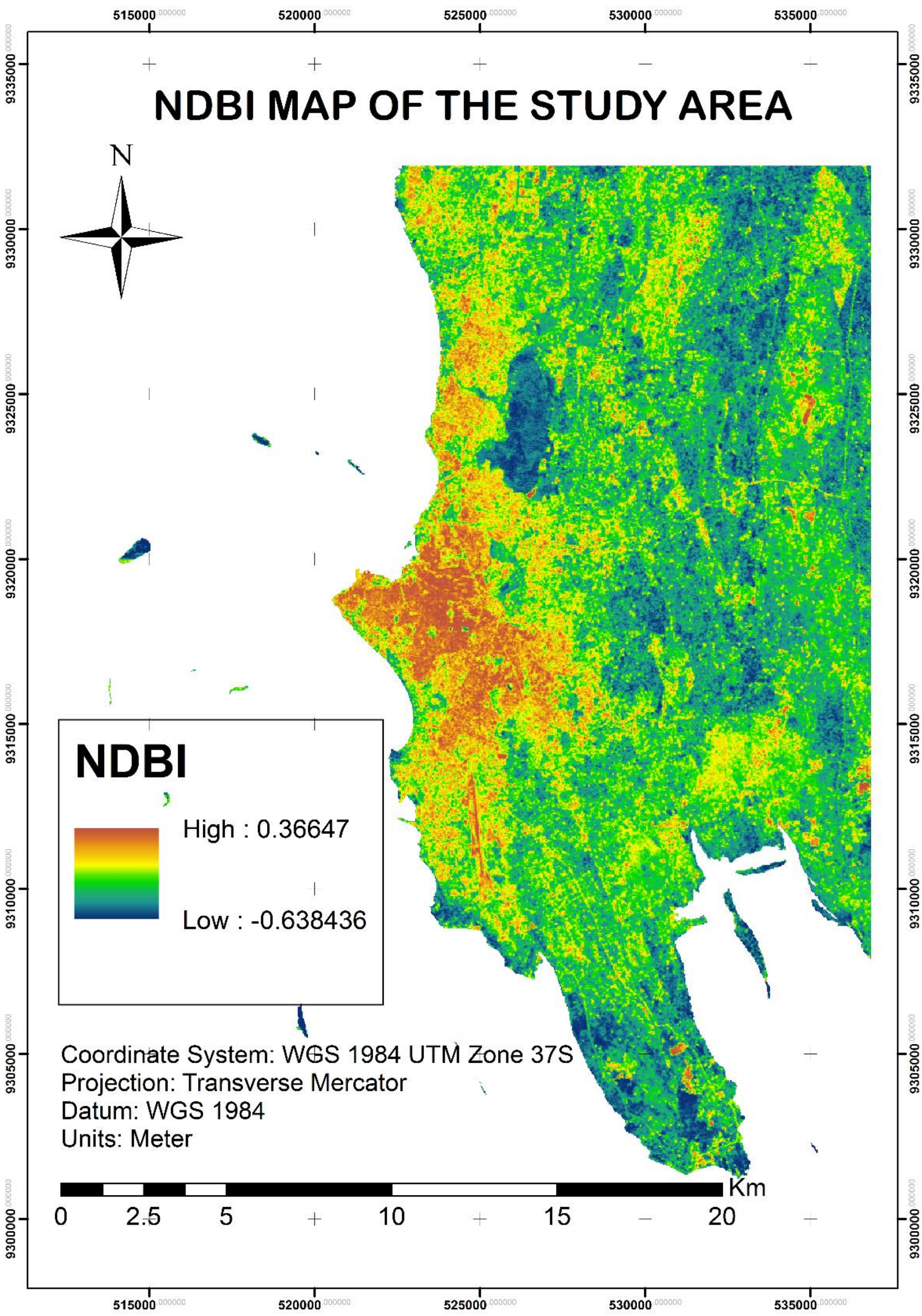

Figure 3.2 NDBI image of the study area using Landsat TM

3.3 Landsat Image Classification

The Landsat images acquired were classified into six (6) distinct classes namely, high vegetated, medium vegetated, low vegetated, bare land, built-up and wetlands. The classification of the images was done using ERDAS IMAGINE image classification and unsupervised classification method was used. Unsupervised classification involves clustering of the pixels to predefined amount of natural spectral clusters based on their DN values and then attaching these clusters to actual land cover classes. These clusters contain pixels which DN values are close as possible to each other and far as possible from other clusters. K-means and Iterative Self-Organizing Data Analysis Technique (ISODATA) are two of the unsupervised classification methods present in ERDAS IMAGINE. In this study ISODATA method was used.

ISODATA unsupervised classification method involves the assessment of the statistics of clusters after each iteration. If the distance between two clusters is lower than predefined minimum they are merged, while if the standard deviation is too high within single cluster it is split to two or the cluster is deleted if the amount of pixel within it is too low. The iteration stops when there are no longer significant changes in the cluster statistics or the maximum number of iterations is reached (Lillesand et al. 2008). The unsupervised classes are solely spectral clusters and on itself they do not refer to any land cover classes, but they can be linked to land covers with reference data which in this study an orthoimage and forest inventory map were used.

In this study, initially, 30 classes were generated which were finally reduced to 6 classes decided to be the final land cover classes. Brief details about supervised and unsupervised classification methods are given in Chapter 1. The classified images were used to identify land-cover types in our study area and also during the analysis of Land Surface Temperatures in their relation with the land cover/use types. The result of this classification is illustrated in Figure 3.3.

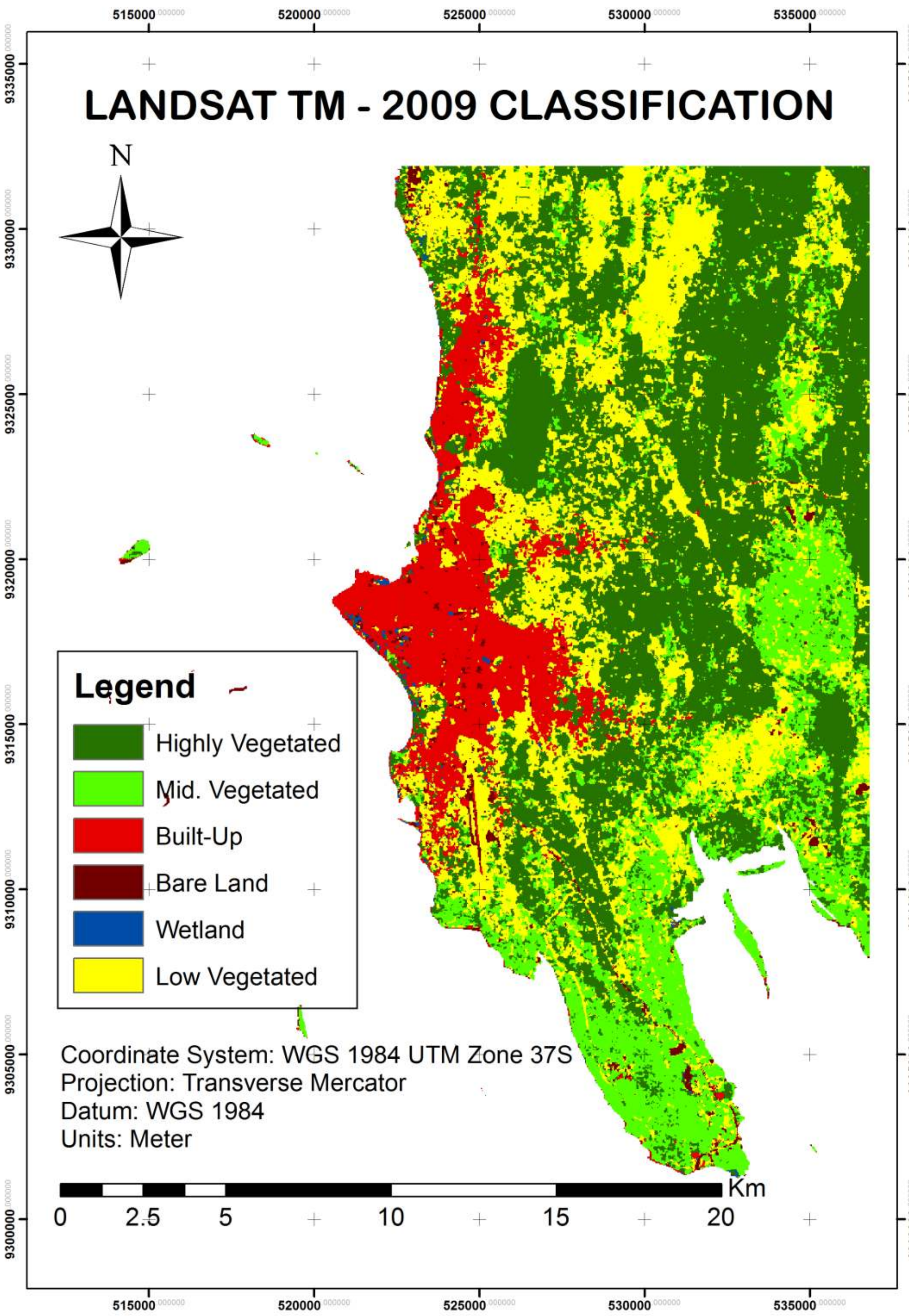

Figure 3.3 Classification of Landsat TM - 2009 image

3.4 Estimation of Land Surface Temperature (LST) Using Landsat TM Data (NDVI Method)

The basis for using Landsat surface temperature is to study the effect of Land-cover/Land-use (LULC) changes in relation to the changes of climate conditions of a place. Land Surface Temperature raster file created in this step was then compared with NDVI and NDBI created in the previous step to establish whether changes in land cover have any effects in the overall changes of local climate. The distribution of LST is consistent with the changes in LULC and the impervious surface (Jiang, Weng, & Fu, 2005). The rational of using NDVI in LST estimation is that the amount of vegetation present is a chief factor, and NDVI can be used to deduce a quick but reliable vegetation conditions of an area. (Weng, Lu & Schubring, 2004). Changes in LULC such as extensive deforestation and rapid urbanization have become chief contributors to climate change and global warming due to remarkable urban heat island (UHI) effect. Researchers have been linking UHI effect to the regional climate, environment, and socio-economic development (Zhang, Odeh & Han, 2009).

The intensity of UHI takes consideration of the temporal dimension of composition of urban areas and vegetation. Hence, the understanding of LST and LULC patterns is essential in sustainable land management and planning (Zhang, Odeh & Han, 2009). The LST of usually have a high correlation with the distribution of land use and land cover (LULC) characteristics (Weng, Lu & Schubring, 2004). The use of NDVI will provide a quick but reliable picture of such correspondence.

There are several methods for Land Surface Temperature estimation, but in this study NDVI method was used. The calculated NDVI was used to estimate the emissivity of an area of interest, which was then used for LST estimation using equation (3.4).

3.4.1 Land Surface Emissivity (LSE)

Emissivity ε is defined as the ratio of the emitted radiance at a given temperature and the blackbody emission at the same temperature. Practically, a material which satisfies the properties of a perfect blackbody does not exist. As a result of this, there is a need of performing a correction to the LSE when deriving LST using remotely sensed data. Therefore, to associate infrared energy radiated by a body with its temperature, the emissivity of such a body has to be known.

The emissivity of a substance is determined by its thermo-physical properties. Thermo-physical properties of an object are used to determine its emissivity. Composition, texture and shape of an object are among the determinants of object emissivity. A relation between NDVI and LSE can be seen as tabulated below s proposed by (Zhang, Wang & Li, 2006). To account for the absorption and atmospheric scattering, atmospheric correction was applied before NDVI calculation.

Table 3.1 LSE classification using NDVI algorithm

NDVI	LSE
NDVI < -0.185	0.995
0.185 ≤ NDVI < 0.157	0.985
0.157 ≤ NDVI ≤ 0.727	1.009 + 0.047 X ln(NDVI)
NDVI > 0.727	0.990

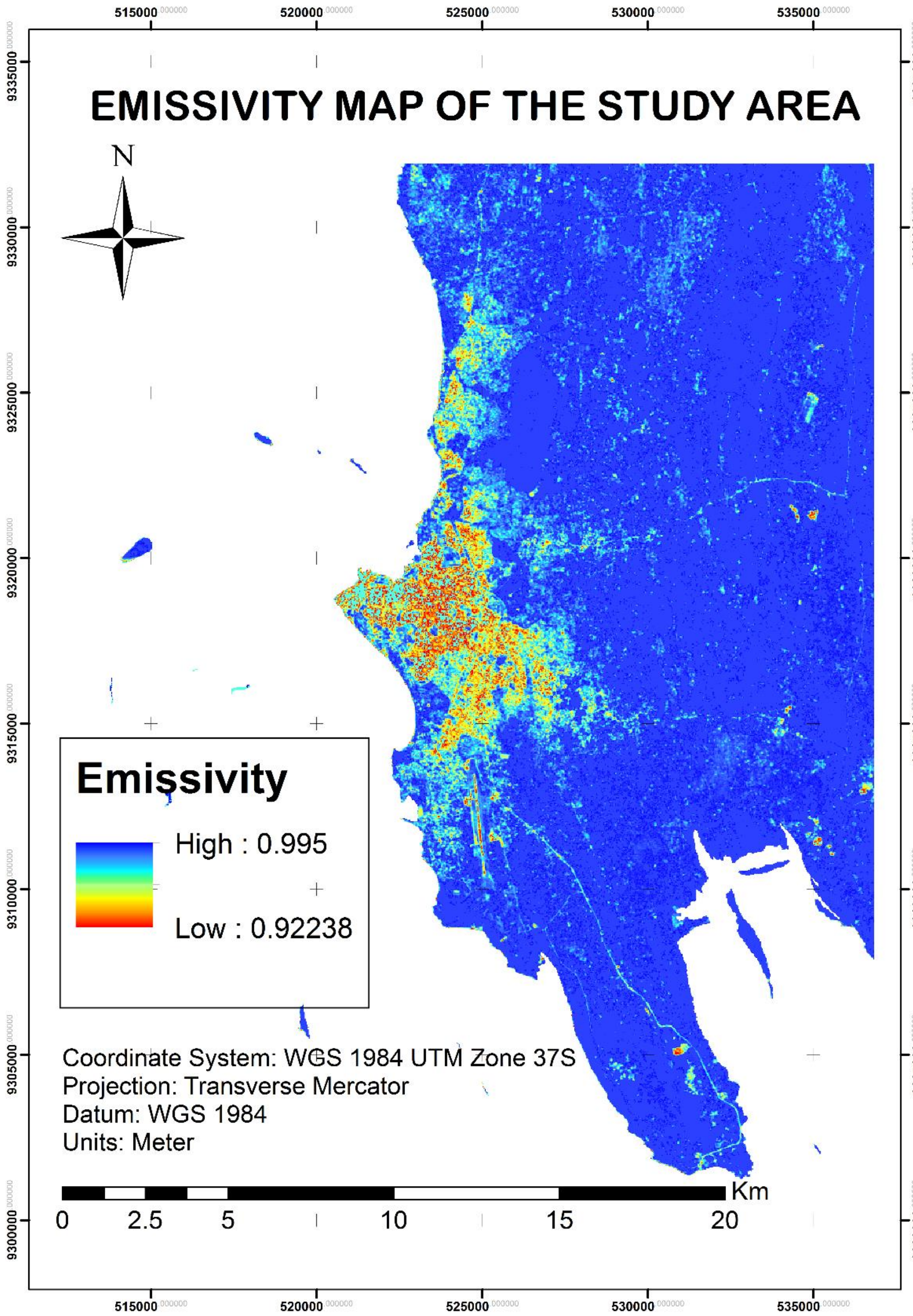

Figure 3.4 Study area emissivity calculated from NDVI image raster

3.4.2 Calculating Brightness Temperature

This step involves the conversion of DN values of the thermal band to obtain effective TOA Brightness Temperature in Kelvin using the below equation.

$$T_B = \frac{K_2}{\ln\left(1 + \frac{K_1}{L_\lambda}\right)} \tag{3.3}$$

where:

T_B – TOA brightness temperature

L_λ – TOA spectral radiance in W/m^2

K_1 – Band- specific thermal conversion constant

K_2 – Band-specific thermal conversion constant

This step is a straight forward conversion using ERDAS IMAGINE 2011, since the software has a module for such conversion. The result of this step was integrated in the final equation for LST estimation.

3.4.3 Estimation of Land Surface Temperature (LST)

The equation (3.4) below incorporates emissivity and brightness temperature developed in the previous two steps to estimate the Land Surface Temperature.

$$S_t = \frac{T_B}{1 + (\lambda \times T_B \,/\, \rho) \ln \varepsilon} \tag{3.4}$$

Where:

S_t – LST

λ – wavelength of emitted radiance (11.5 μm for Landsat TM)

ρ – h * c / σ (1.438 x 10^{-2} mK)

σ – Stefan Boltzman constant (5.67 x 10^{-8} Wm^{-2} K^{-4})

c – light speed (2.998 x 10^{8} m/s)

h – Planck's constant (6.6626 x 10^{-34} J s)

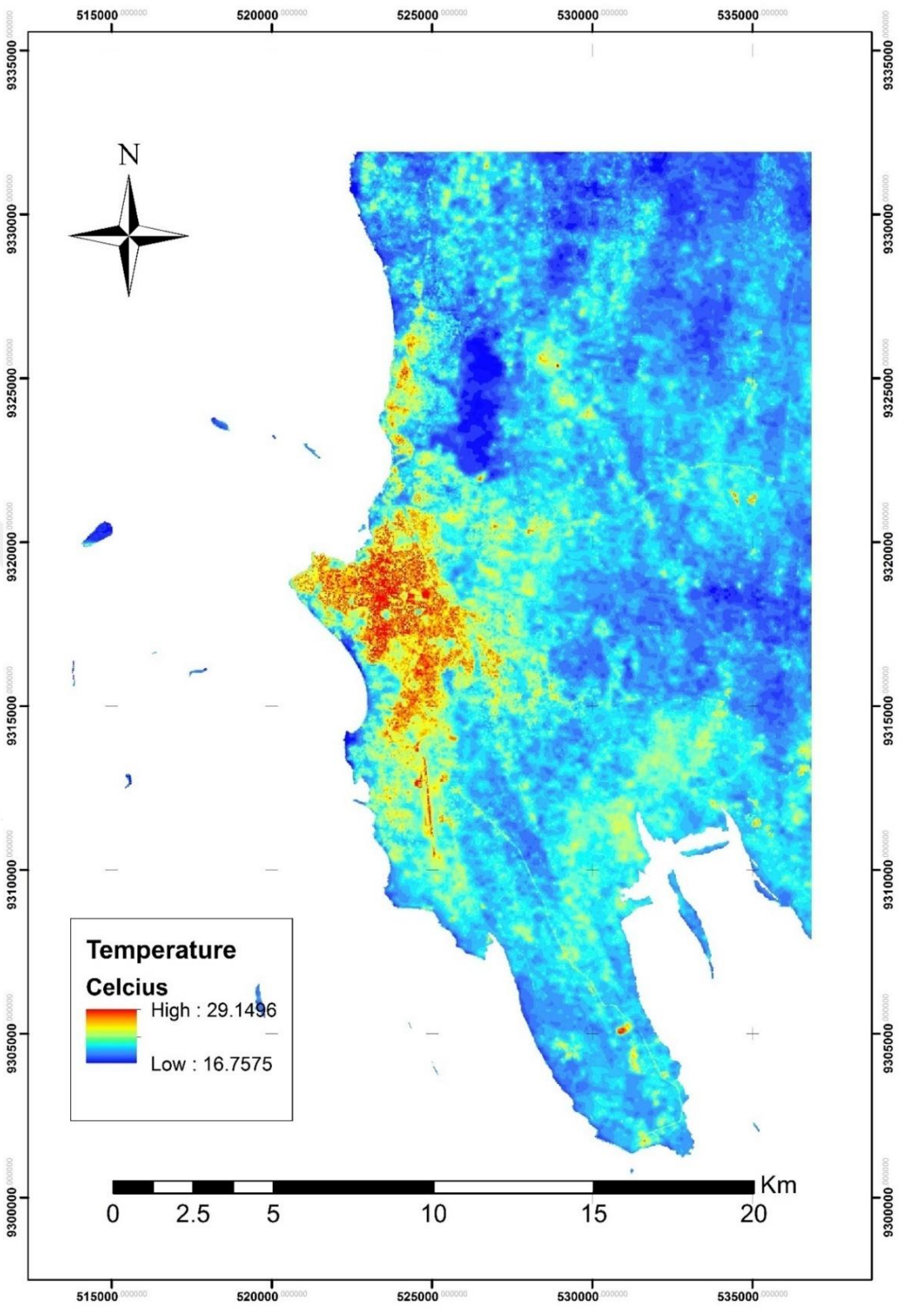

Figure 3.5 LST image of the study area

CHAPTER FOUR
RESULTS AND ANALYSIS

4.1 LST, NDVI and NDBI Relationship

The results of NDVI and NDBI calculations can be seen as represented in maps shown in Figure 3.1 and Figure 3.2 and respectively. Figure 3.5 shows the map of our study area depicting spatial distribution of LST. Statistical calculations show that the NDVI values varied from – 0.4250 to 0.9206 with mean value of 0.6754 which signifies that our study area is pretty well vegetated. The values of NDBI range from – 0.684 to 0.3665 with a mean value of – 0.2209. The calculated LST raster had values ranging from 16.7575 to 29.1496 with an average of 20.4013.

The indices created before i.e. NDVI and NDBI were then plotted against LST to study the correlation (pixel by pixel) between land-cover and changes in temperature of an area. The graph shows a high correlation between LST and NDBI in our study area. The correlation coefficient of $R^2 = 0.7637$ shows a very positive correlation between the increase of temperature and development of built-up areas. This signifies that the more urbanized an area is, the higher its temperature readings will be.

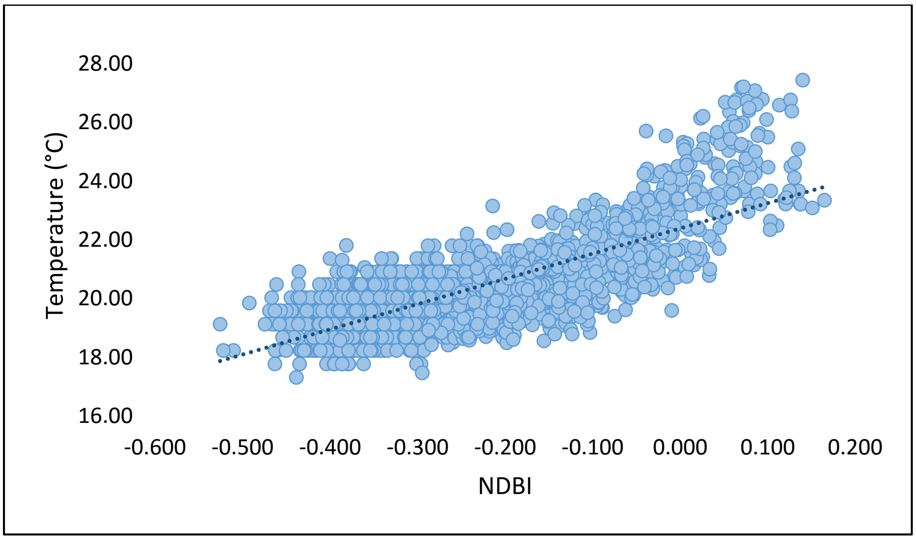

Figure 4.1 The relationship between LST and NDBI

On the other hand, LST and NDVI correlation have produced negative value of $R^2 = -0.7983$, that signifies that the more vegetated an area is, the less temperature would be recorded. That means highly vegetated areas and areas with forest covers accumulate less heat and hence lower temperature readings.

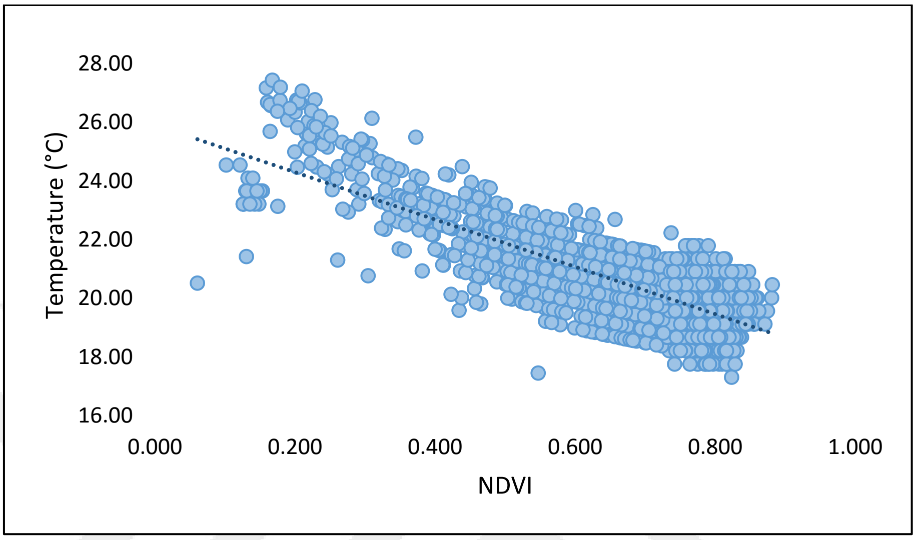

Figure 4.2 The relationship between LST and NDBI

This is proven by plotting NDBI against NDVI as seen in Figure 4.3 The relationship between NDBI and NDVI ha NBDI depicts a strong negative correlation value of $R^2 = -0.8820$, which makes sense, since barren land and built up areas are not vegetated and therefore the values taken from same point will be completely reversed for each index.

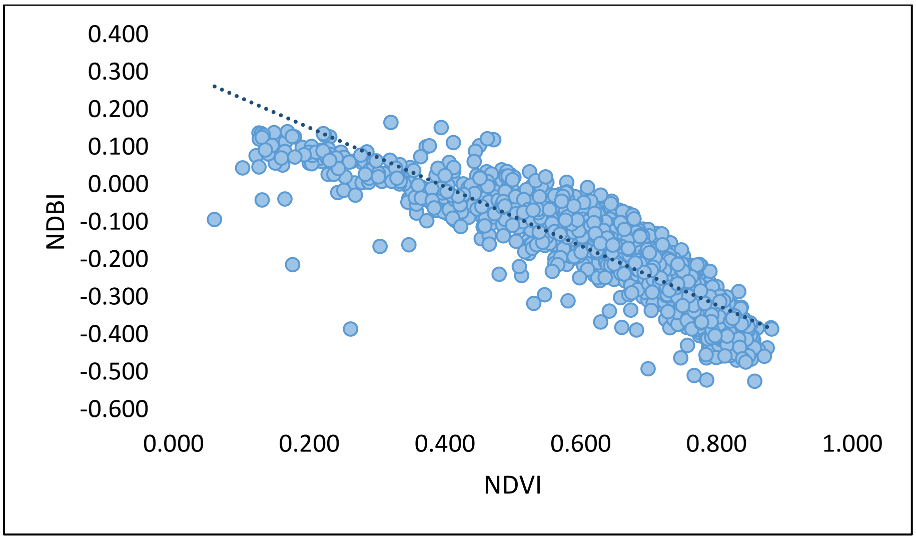

Figure 4.3 The relationship between NDBI and NDVI

4.2 Land-cover Types and LST Relationship

This section analyses the relationship between each individual land-cover's composition, distribution and quantity against the LST.

The classification of Landsat TM image of July 2009 identified five major land cover categories in that year namely, high vegetated, medium vegetated, low vegetated, built-up area, bare land and wetlands. Each land-cover type represents some distinct attributes in both composition and characteristics. The total study area which includes some surrounding islets, covers a total area of 34275 ha. The result of this classification of the images found that highly vegetated land cover type in the study area covers an area of 14,800 ha, which is equal to 43.18 % accounting for the largest area in the study area. Medium vegetated land cover occupies 5,800 ha which is around 16.92 %of the total area. Low vegetated area covers 9,171 ha equalling 26.76 % of the total land cover. Built-up area covers an area of 3865 ha accounting for 11.28 % of total land cover in the study area, whereas, another non-vegetated land-cover type, bare land, covers only 512 which is equal to 1.49 %. Wetlands covers merely, 127 ha which is only 0.37 % of the total area.

Table 4.1 Landsat TM -2009 classification in the study area

LULC Type	Area in hectares (ha)	Percentage Cover (%)
High Vegetated	14800	43.18
Medium Vegetated	5800	16.92
Low Vegetated	9171	26.76
Built-up	3865	11.28
Bare land	512	1.49
Wetlands	127	0.37
Total	**34275**	**100**

The LULC types in 2009 were compared with the LST of the study area with results summarized in Table 4.2. These results illustrate how different land use/cover types dissipate heat and temperatures differently resulting with each land cover type having different average temperatures. From the Table 4.2 it can be clearly deduced that highly vegetated areas i.e. forested areas, agroforests and mixed plantations, have registered minimum average temperatures of 19.6870 °C followed by medium vegetated areas which consist mainly of coral rags and scrubs, recording 19.9809 °C, low vegetated i.e. farmlands, paddy fields and large fields, have average temperatures of 20.8064 °C. The trend continues as wetlands recorded average temperatures of 20.8350 °C slightly higher than the vegetated land-covers. Bare land has an average temperature of 22.5793 °C lower than the built-up areas which exhibit the highest radiant average temperatures among the land-cover types in our study with average temperatures of 23.0573 °C.

Table 4.2 Descriptive statistics of LST against land cover/use for the study area

Land cover	**MIN**	**MAX**	**MEAN**
High Vegetated	16.8536	23.7952	19.6870
Medium Vegetated	16.8536	22.7017	19.9809
Built-up	16.7575	29.1496	23.0573
Bare land	17.3066	28.9847	22.5793
Wetlands	17.1362	25.4426	20.8350
Low Vegetated	17.5748	28.5517	20.8064

It can be also presumed that the less vegetated the land-cover the lower its temperature will be. This infers that urbanization and deforestation does bring up LST by replacing natural vegetation with non-evaporating, non-transpiring surfaces such as bricks, metal, tarmac and concrete. This is evident as maximum temperatures for built-up areas is 29.1496 °C nearly 5 points higher than that of high vegetated area at 23.7952 °C.

CHAPTER FIVE
CONCLUSIONS AND DISCUSSION

The results of this study clearly shows the effect of land cover types identified using classification methods and vegetation indices (i.e. NDVI and NDBI) to the climate conditions of place. Non-vegetated areas recorded high temperatures compared to vegetated land covers. The analysis used only one dimension of climate attribute i.e. temperature, yet the changes of temperature have been confirmed to affect both rainfall formation and wind regimes since temperatures also tend to affect atmospheric pressure which in turn has an effect on wind formations. Lack of data restricted a comparison that would have been made, that would compare satellite images collected from different dates and study how their changes affect the LST. Studies have demonstrated that the direct effect of land use/cover changes on one environmental element can cause indirect effect on the other. The increase of surface temperature was related to the decrease of vegetated and the vice versa is true (Weng, 1999).

Despite the fact that the methodology used in this study measures only one aspect of climate element i.e. LST in relation to in land-cover, yet it was enough to provide evidence that the changes between LULC, vegetation indices and LST do correlate and have effects on each other. Therefore, proper management of land and their change pattern could help in minimizing the effect of the changing climate. It is clear from the analysis, vegetated areas are susceptible to low temperatures whereas, more heat is absorbed in non-vegetated areas especially built-up areas where temperature reading are usually high.

Previous studies done on Unguja island indicates that the highly vegetated areas are decreasing by an alarming rate, which are either replaced by barren land, built-up area due to population increase or by agricultural lands. The non-vegetated or low vegetated land-covers as seen from the analysis of this study tend to measure high temperatures, a phenomenon that would result to an increase of overall temperatures on the island.

According to Kukkonen (2013) annual forest cover change on Unguja island is between - 0.82% and -1.19%, he also deduced that an estimate of only 485 km^2 of forest cover on Unguja island will be left by the year 2025 from a total of 572 km^2, where much of the deforestation is expected to take place along the coastline. Research done by Senga et al. (2014) in Bumbwini and Kisakasaka found that there was a decrease of mangroves and mixed tress covers in those areas and an increase of bare lands and rice pads. Both results imply that much of the land will be covered by heat absorbing land covers such as built-up areas, agricultural lands and/or barren lands that will increase the LST and overall temperatures of Zanzibar. This coupled with other factors such as increase of sea surface temperature and negative effects of population increase such as deforestation and intense urbanization will further exacerbate the problem.

These results are expected to provide a starting point for planers and policy makers in Zanzibar to identify the types of land covers that require dedicated intervention and protection from undergoing further changes. This means high vegetated areas such as forests, mixed plantations and agroforests need to be preserved and protected against deforestation and intense urbanization. Afforestation and reforestation should be encouraged especially along the coastline (e.g. mangrove and sea grasses afforestation) to reduce the temperatures on the island, they will also help in absorbing excess carbon dioxide in the atmosphere and act as a shoreline protection against high tides and strong winds due to changes in ocean currents and wind regimes. Policies that would discourage intense urbanization should be enacted and their implementation should be insured to reduce the conversion of vegetated areas into heat-absorbing non-vegetated surfaces, hence decrease the overall temperatures. Even with the current trends proper management of land will help to reduce and mitigate some of the negative effects of climate change in Zanzibar.

Further study is needed to provide a much clearer picture as to what extent changes of land cover types is affecting the climate of Zanzibar as far as climate change and global warming is concerned. Lack of both satellite data due to heavy clouds formation all year long and lack of metrological data for comparison of remote sensing techniques and locally collected data was a huge setback in this study. However, several studies such as a study by Zhang et al. (2009) on the use remote sensing technology to quantify climate conditions of the earth have confirmed the reliability of the method used in this study.

REFERENCES

Ali, H. R., Nyakairu, G. W., & Vuai, S. A. (2012). Influence of tides to the cave water quality: a case study on Zanzibar Island, Tanzania. *International Journal of Current Research*, 327 - 334.

Boko, M., Niang, I., Nyong, A., Vogel, C., Githeko, A., Medany, M., Osman-Elasha, B., Tabo, R., & Yanda, P. (2007). *Africa. climate change 2007: Impacts, adaptation and vulnerability. contribution of working Group II to the fourth assessment report of the intergovernmental panel on climate change.* Cambridge: Cambridge University Press.

Brown, O., Hammill, A., & MacLeman, R. (2007). Climate change as the 'new' security threat: implications for Africa. *International Affairs, LXXXIII*(6), 1141–1154.

Brown, S., Kebede, A. S., & Nicholls, R. J. (2011). *Sea-level rise and impacts in Africa, 2000 to 2100.* University of Southampton, School of Civil Engineering and the Environment, Southampton.

Chavez, P. S. (1988). An improved dark-object subtraction technique for atmospheric scattering correction of multispectral data. *Remote Sensing of Environment*, 459-479.

Chavez, P. S. (1989). Radiometric calibration of landsat thematic mapper multispectral images. *Photogrammetric Engineering and Remote Sensing, LV*(9), 1285-1294.

Chavez, P. S. (1996). Image-based atmospheric corrections - revisited and improved. *Photogrammetric Engineering & Remote Sensing*, 1025-1036.

Confalonieri, U., Confalonieri, U., Menne, B., Akhtar, R., Ebi, Kristie L.; Hauengue, M., Kovats, R. S., Revich, B., & Woodward, A. (2007). *Human health. Climate change 2007: Impacts, adaptation and vulnerability. Contribution of working* *group II to the fourth assessment report of the intergovernmental panel on climate change.* Cambridge: Cambridge University Press.

Doney, S., Rosenberg, A., Alexander, M., Chavez, F., Harvell, C. D., Hofmann, G., Orbach, M., & Ruckelshaus, M., (2014). *Chapter 24: oceans and marine resources. Climate change impacts in the United States: The third national climate assessment.* U.S. Global Change Research Program.

Du, Y., Teillet, P. M., & Cihlar, J. (2002). Radiometric normalization of multitemporal high-resolution satellite images with quality control for land cover change detection. *Remote Sensing of Environment*, 123–134.

United States Environmental Protection Agency [EPA]. (2015). *Climate change indicators in the United States*. Retrieved February 5, 2016, from http://www3.epa.gov/climatechange/science/indicators/snow-ice/sea-ice.html

United States Environmental Protection Agency [EPA]. (2014). *Climate change indicators in the United States.* United States Environmental Protection Agency.

Food and Agriculture Organization [FAO]. (2005). *The state of food and agriculture.* Rome: FAO.

Green, E. P., Clark, C. D., Mumby, P. J., Edwards, A. J., & Ellis, A. C. (1998). Remote sensing techniques for mangrove mapping. *International Journal of Remote Sensing*, 935 - 956.

Groffman, P. M., Kareiva, P., Carter, S., Grimm, N. B.; Lawler, J., Mack, M., Matzek, V., & Tallis, H. (2014). *Chapter. 8: Ecosystems, biodiversity, and ecosystem services. Climate change impacts in the United States: The Third National Climate Assessment.* U.S. Global Change Research Program.

Guanter, L., Ritcher, R., & Kaufamann, H. (2009). On the application of the MODTRAN4 atmospheric radiative transfer code to optical remote sensing. *International Journal of Remote Sensing*, 1407 - 1424.

Herschel, W. (1801). Observations tending to investigate the nature of the sun, in order to find the causes or symptoms of its variable emission of light and heat; With remarks on the use that may possibly be drawn from solar observations. *Philosophical transactions of the Royal Society of London.*, 265-318.

Hettige, P. M. (1990). *Land evaluation and land suitability classification Unguja & Pemba Islands.* Food And Agriculture Organization of The United Nations. FAO.

Huete, A. R. (1988). *A soil-adjusted vegetation index (SAVI).* Remote Sensing of Environment.

Intergovernmental Panel on Climate Change (IPCC). (2013). *Climate change 2013: The physical science basis. Working Group I contribution to the IPCC Fifth Assessment Report.* Cambridge, United Kingdom: Cambridge University Press.

Intergovernmental Panel on Climate Change (IPCC). (2007). *Climate change 2007: mitigation.* New York: Cambridge University.

Jensen, J. R. (2000). *Remote sensing of the environment: an earth resource perspective.* U.S.A: Pearson.

Jensen, J. R. (2005). *Introductory digital image processing: a remote sensing perspective* (3rd ed.). U.S.A: Prentice Hall.

Jevrejeva, S., Moore, J. C., & Grinsted, A. (2012). Sea level projections to AD2500 with a new generation of climate change scenarios. *Global and Planetary Change*, 14–20.

Jiang, Y., Weng, Q., & Fu, P. (2005). Assessing the impacts of urbanization-associated land use/cover change on land surface temperature and surface moisture: a case study in the Midwestern United States. *Remote Sensing*, 4880-4898.

Kukkonen, M. (2013). *Forest cover and its change in Unguja Island, Zanzibar*. Master's Thesis, University of Turku, Finland.

Li, H., & Liu, Q. (2008). Comparison of NDBI and NDVI as indicators of surface urban heat. *International Conference on Earth Observation Data Processing and Analysis.*

Li, H., & Liu, Q. (2008). Comparison of NDBI and NDVI as indicators of surface urban heat island effect in MODIS imagery. *International Conference on Earth Observation Data Processing and Analysis.*

Lu, D., Mausel, P., Brondizio, E., & Moran, E. (2004). Change detection techniques. *Internationa Journal of Remote Sensing*, 2365–2407.

Mas, J. F. (1999). Monitoring land-cover changes: a comparison of change detection techniques. *International Journal of Remote Sensing*, 139 - 152.

Mbilinyi, A., Saibul, G. O., & Kazi, V. (2013). *Impact of climate change to small scale farmers: Voices of farmers in village communities in Tanzania.* Economic and Social Research Foundation.

NASA's Jet Propulsion Laboratory. (2016). *A blanket around the Earth*. Retrieved from NASA: Global Climate Change: http://climate.nasa.gov/causes/

Newhall, C., Hendley, J. W., & Stauffer, H. (1997). *Benefits of volcano monitoring far outweigh costs —the case of Mount Pinatubo.* United States Geological Survey.

Nicholls, R. J., Wong, P., Burkett, V., Codignotto, J., Hay, J., McLean, R., Ragoonaden, S., Woodroffe, R., & Colin D. (2007). *Coastal systems and low-lying areas. Climate Change 2007: Impacts, adaptation and vulnerability. contribution of working group II to the fourth assessment report of the intergovernmental panel on climate change.* Cambridge: Cambridge University Press.

National Oceanic and Atmospheric Administration. (2015). *What is remote sensing?* Retrieved February 12, 2016 from http://oceanservice.noaa.gov/facts/remotesensing.html

Office of Chief Government Statistician. (2014). *Basic demographic and socio-economic profile, Tanzania Zanzibar.* Zanzibar: Ministry of State Zanzibar.

Oliver, J. E., & Fairbridge, R. W. (1987). *The Encyclopedia of climatology*. New York: Van Nostrand Reinhold.

Paavola, J., & Adger, W. N. (2002). *Justice and adaptation to climate change.* Tyndall Centre for Climate Change Research.

Ramirez, M. (2012). *Volcano Tombora.* Retrieved June 29, 2016 from https://prezi.com/d8yrqzyjwiex/volcano-tombora/

Richards, J. A., & Jia, X. (2006). *Remote sensing digital: an introduction.* Germany. Springer.

Robock, A. (2002). Volcanic eruption, El chich´on. *the earth system: Physical And Chemical Dimensions of Global Environmental Change*, 736–736.

Roschina, E. M., & Sarychev, A. P. (2010). Spörer's law and rythm of sunspot cycles. *Solar System Research*, 376 - 382.

Rouse, J. W., Haas, R. H., Schell, J. A., & Deering, D. W. (1973). Monitoring vegetation systems in the Great Plains with ERTS. *Third ERTS Symposium*, 309-317.

Schowengerdt, R. A. (2006). *Remote sensing: models and methods for image processing.* United States of America. Academic Press.

Senga, H. O., Kihupi, N. I., Liwa, E., & Kimaro, D. (2014). Land cover changes along the coastal marine ecosystems of Zanzibar. *Journal of Asian Scientific Research*, 83-98.

Shlionskaya, I. (2011). *Solar cycle to cause global natural disasters?* Retrieved August 16, 2016, from Truth Theory: http://truththeory.com/2011/12/30/solar-cycle-to-cause-global-natural-disasters/

Singh, A. (1989). Review article digital change detection techniques using remotely-sensed data. *International Journal of Remote Sensing*, 989-1003.

Song, C., Woodcock, C. E., Seto, K. C., Lenney, M. P., & Macomber, S. A. (2001). Classification and change detection using Landsat TM data. *Remote Sensing of Environment*, 230–244.

Stocker, T. F., Qin, D., Plattner, G., Tignor, M., Allen, K., Boschung, J., Nauels, A., Xia, Y., Bex, V., & Midgley, M. (2013). *IPCC, 2013: Climate change 2013: the physical cience basis. Contribution of working group I to the fifth assessment report of the intergovernmental panel on climate change.* Cambridge: Cambridge University Press.

The Revolutionary Government of Zanzibar. (2007). *Zanzibar Strategy for Growth and Reduction of Poverty.* Zanzibar.

United States Geological Survey [USGS]. (2015). *Landsat - earth observation satellites.* Reston, VA: United States Geology Survey.

United States Geological Survey [USGS]. (2015). *Landsat 8*. Retrieved March 23, 2016 from http://landsat.usgs.gov/landsat8.php

United State Geological Survey [USGS]. (2012). *Historical perspective.* Retrieved July 2, 2016 from http://pubs.usgs.gov/publications/text/historical.html

Walsh, J., Wuebbles, D., Hayhoe, K., Kossin, J., Kunkel, K., Stephens, G., Thorne, P., Vose, R., Wehner, M., Willis, J., Anderson, D., Doney, S., Feely, R., Hennon, P., Kharin, V., Knutson, T., Landerer, F., Lenton, T., Kennedy, J., & Somerville, R. (2014). *Chapter 2: Our changing climate. Climate change impacts in the United*

States: The third national climate assessment. U.S. Global Change Research Program. J. M. Melillo, Terese (T.C.) Richmond, and G. W. Yohe, Eds.

Wang, Y., Tobey, J., Bonynge, G., Nugranad, J., Makota, V., Ngusaru, A., & Traber, M. (2005). Involving geospatial information in the analysis of land-cover change along the tanzania coast. *Coastal Management*, 89–101.

Weng, Q. (1999). A remote sensing–GIS evaluation of urban expansion and its impact on surface temperature in the Zhujiang Delta, China. *International Journal of Remote Sensing*, 1999–2014.

Weng, Q., Lu, D., & Schubring, J. (2004). Estimation of land surface temperature–vegetation abundance relationship for urban heat island studies. *Remote Sensing of Environment*, 467–483.

Wilbanks, T., Lankao, P., Bao, M., Berkhout, F., Cairncross, S., Ceron, J., Kapshe, M., Muir-Wood, R., & Zapata-Marti, R. (2007). *Industry, settlement and society. Climate change 2007: impacts, adaptation and vulnerability. Contribution of working group II to the fourth assessment report of the intergovernmental panel on climate change.* Cambridge: University Press.

Williams, D. R. (2016). *Sun fact sheet.* Retrieved June 29, 2016 from http://nssdc.gsfc.nasa.gov/planetary/factsheet/sunfact.html

Xu, H. (2007). Extraction of urban built-up land features from landsat imagery using a thematic-oriented index combination technique. *Photogrammetric Engineering & Remote Sensing*, 1381–1391.

Zhang, J., Wang, Y., & Li, Y. (2006). A C++ program for retrieving land surface temperature from the data of Landsat TM/ETM+ band6. *Computers & Geosciences*, 1796–1805.

Zhang, Y., Odeh, I. O., & Han, C. (2009). Bi-temporal characterization of land surface temperature in relation to impervious surface area, NDVI and NDBI, using a subpixel image analysis. *International Journal of Applied Earth Observation and Geoinformation*, 256–264.

APPENDICES

APPENDIX A: ACRONYMS

CSIRO	: Commonwealth Scientific and Industrial Research Organisation
EPA	: United States Environmental Protection Agency
ESA	: European Space Agency
FAO	: Food and Agriculture Organization of the United Nations
GIS	: Geographic Information Systems
IPCC	: Intergovernmental Panel on Climate Change
JMA	: Japan Meteorological Agency
LST	: Land Surface Temperature
NASA	: National Aeronautics and Space Administration
NDBI	: Normalized Difference Built-up Index
NDVI	: Normalized Difference Vegetation Index
NOAA	: National Oceanic and Atmospheric Organization
NSIDC	: National Snow and Ice Data Center
MRI	: Meteorological Research Institute
TMA	: Tanzania Metrological Agency
WRI	: World Resources Institute